Technische Universität Braunschweig
Leichtweiß-Institut für Wasserbau
Abteilung Hydromechanik und Küsteningenieurwesen
Prof. Dr.-Ing. Hocine Oumeraci

LWI Bericht Nr. 942

Numerical Simulations on the Stability of Coastal Structures made of Geotextile Sand Containers (GSC)

DAAD Stipendiat M.Sc. Juan Recio
Professor Dr.-Ing. Hocine Oumeraci

BRAUNSCHWEIG
May 2007

Beethovenstraße 51a · 38106 Braunschweig · Telefon: 0531/391 3930 · Fax: 0531/391 8217
E-Mail: h.oumeraci@tu-bs.de · www.lwi.tu-bs.de

"Coupled" Numerical Simulations on the Stability of Coastal Structures made of Geotextile Sand Containers (GSC)

TABLE OF CONTENTS **Page**

1. Description of Numerical Models used for Simulations 1
    1.2 Flow Model 1
    1.1 Structural Dynamic Models 1
        1.2.1 Brief Description of "UDEC" 2
        1.2.2 Block (Element) Constitutive Models in UDEC 2
        1.2.3 Displacemet Model in UDEC 3
        1.2.4 Dynamic Analysis in UDEC 3
        1.2.5 Modifications Performed to UDEC 3

2. Partial "Coupling" of the Models (Cobras-UDEC) 3
    2.1 Further Details of the Partial Coupling 5
    2.2 Tolerance for Updating the Structure Geometry in "Cobras" 6

3. Application of the "Coupled" Model to the Stability of GSC-Structures 7
    3.1 Application of the "Coupled" Model to the Model Tests Performed by Hinz and Oumeraci 2002 9
    3.2 Brief Description of the GSC-Structure and Model Tests presented by Hinz and Oumeraci 2002 10
    3.3 Definition of Computational Domain for the Flow and Structural Models 10
    3.4 Additional Considerations for Simulating the GSCs 12
    3.5 Constitutive Model for the Deformation of the GSCs 14
    3.6 Input Parameters for the Numerical Simulations 14

4. "Coupled" Simulations Results 15

5. Numerical Simulations and Analysis of the Stability of GSC-Structures 19
    5.1 Wave-Induced Deformation on GSCs 19
    5.2 Wave-Induced Stresses inside GSCs 22
    5.3 Influence of Boundary Conditions on Hydraulic Stability 22
    5.4 Friction between Neighbouring Containers 25

6. Full Coupling of the Model 25

7. Concluding Remarks 26

8. Annexes and References 27

"Coupled" Numerical Simulations on the Stability of Coastal Structures made of Geotextile Sand Containers (GSC)

Introduction

This is the second part of the report "Hydraulic Processes Associated with the Instability of GSC-Structures –A numerical Study Using "Cobras"- (Recio and Oumeraci 2006). In this second part the "Cobras" model is used to provide the wave-induced pressures around GSCs to simulate the stability of coastal structures made of GSCs under wave action by using two numerical structural models (FEM and DEM,). The numerical results are qualitatively and quantitatively compared with experimental data. The report is divided in the following sections: (i) brief description of the numerical models used for the simulations, (ii) "coupling" of the models, (iii) adaptation of the models for simulating the stability of GSC-structures, (iv) comparison of results of numerical simulations and experimental data and (v) numerical simulations to investigate the processes affecting the stability of GSC-structures.

1. Description of Numerical Models Used for Simulations

Given the complexity of the forces acting on GSC-structures and considering all the processes affecting the stability, numerical modelling represents an appropriate mean to cope with all the involved processes and their interactions. For this purpose a flow model (VOF) and two coupled structural models (FEM/DEM) are required. These three models (VOF-FEM-DEM) are partially "coupled" and used for the simulation of GSC-structures under wave action.

1.1 Flow Model

As mentioned by Recio and Oumeraci (2006), the most suitable way of obtaining numerically the wave-induced pressures acting on GSCs is to apply the "Cobras" model which is a Volume of Fluid (VOF) type model based on the Reynolds Averaged Navier Stokes equations (RANS) originally developed by the research team of Professor P. L F Liu from Cornell University, Ithaca, USA.
"Cobras" (**Co**rnell **Br**eaking Waves **a**nd **S**tructures) is a numerical model for calculating the evolution of a breaking wave and its interaction with structures.
More details on the "Cobras" model can be found in Recio and Oumeraci (2006) and Liu and Lin (1999) and Liu and Lin (1998).

1.2 Structural Dynamic Models

A coupled FEM-DEM (finite element method and discrete element method) is the most appropriate to simulate numerically the behaviour of GSC-structures under wave action. This can be explained due to the deformations and displacements that the elements experience, which cannot be described by a single FEM model.

Therefore, the FEM simulates both deformations and stresses while the DEM describes the displacement and contact detection between GSCs.
Due to time limitations, a commercially available numerical model named "UDEC", which is a coupled FEM-DEM model was used for this study. Developing a coupled FEM-DEM from "scratch" would be unfeasible considering the time frame available. A brief description of the FEM and DEM methods is explained in Annexes 1 and 2.

1.2.1 Brief description of "UDEC"

The **U**niversal **D**istinct **E**lement **C**ode (UDEC) is a two-dimensional numerical program based on the distinct element method for discontinue modelling. UDEC simulates the response of discontinuous media subjected to either static or dynamic loading. The discontinuous medium is represented as an assemblage of discrete blocks or elements. The discontinuities are treated as boundary conditions between blocks (elements); large displacements along discontinuities and rotations of blocks are allowed. Individual blocks behave either as rigid or deformable material. Deformable blocks are subdivided into a mesh of finite-difference elements, and each element responds according to a prescribed linear or non-linear stress-strain law. The relative motion of the discontinuities is also governed by linear or non-linear force-displacement relations for movement in both the normal and shear directions.

1.2.2 Block (Element) Constitutive Models in UDEC

There are seven constitutive models provided in UDEC for representing the deformation of blocks (elements): 1) null model (for removed blocks), 2) elastic, isotropic model, 3) Drucker-Prager model, 4) Mohr-Coulomb model, 5) ubiquitous-joint model, 6) strain-softening model and 7) double-yield model. Figure 1 shows the yield surfaces of the two most used constitutive models in UDEC (Mohr-Coulomb and Drucker-Prager).

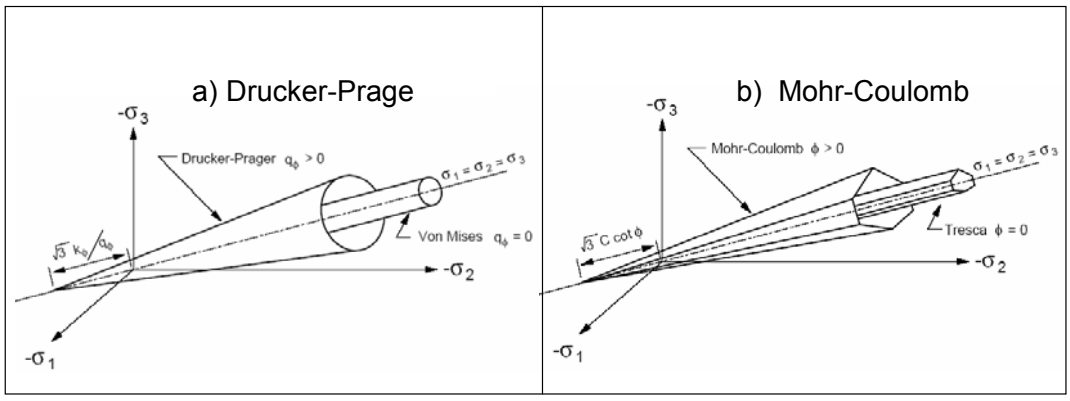

Figure 1: Drucker-Prager (a) and Mohr-Coulomb (b) Yield Surfaces in Principal Stress Space (after Itasca 2004)

1.2.3 Displacement Model in UDEC

This model uses the "Coulomb frictional behaviour" and refers to the capability of UDEC to simulate displacement of each block (element) in all directions where a discontinuity (or gaps) exists. The displacement model of UDEC is intended to simulate the individual displacement of blocks under shear. Friction coefficient between blocks and roughness parameter are the main parameters in the displacement model. Figure 2 shows the basic gap behaviour model in UDEC.

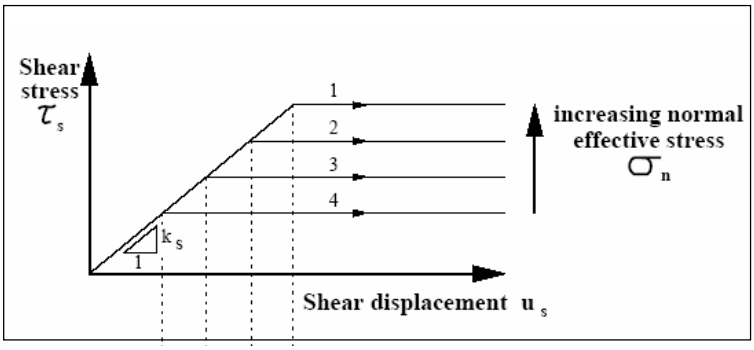

Figure 2: Discontinuity Behaviour Model in UDEC (after Itasca 2004)

1.2.4 Dynamic Analysis in UDEC

Dynamic analysis in UDEC permits two-dimensional, plane-strain or plane-stress, fully dynamic analysis. The calculation is based on the explicit finite difference scheme to solve the full equations of motion. In UDEC, the dynamic input can be applied in one of the following ways: a) a velocity history, b) a stress history, c) a force history and a d) fluid pressure history.
More details on the UDEC model can be found in Itasca 2004.

1.2.5 Modifications Performed to UDEC

The UDEC model has been extended in the following ways:

a) The model was extended to allow different zones with different properties inside an element (see section 3.4 for details).
b) The model was adapted to be capable to read output files created by "Cobras".

2. Partial "Coupling" of the Models (Cobras-UDEC)

Due to time limitations and feasibility aspects, only a "partial coupling" of "Cobras" and "UDEC" was required within the time available. "Cobras" and "UDEC" have been run independently, only sharing input and output information among them. Ideally, the models (fluid and structural dynamic models) should run simultaneously, sharing continuously and instantaneously information. Therefore, partial coupling might represent a serious limitation in the following cases: (i) a

detached element is "floating" away from the structure, (ii) displacement of several elements occur simultaneously, and (iii) deformations during a time step are large enough to affect considerably and immediately the boundary conditions of neighbouring elements.

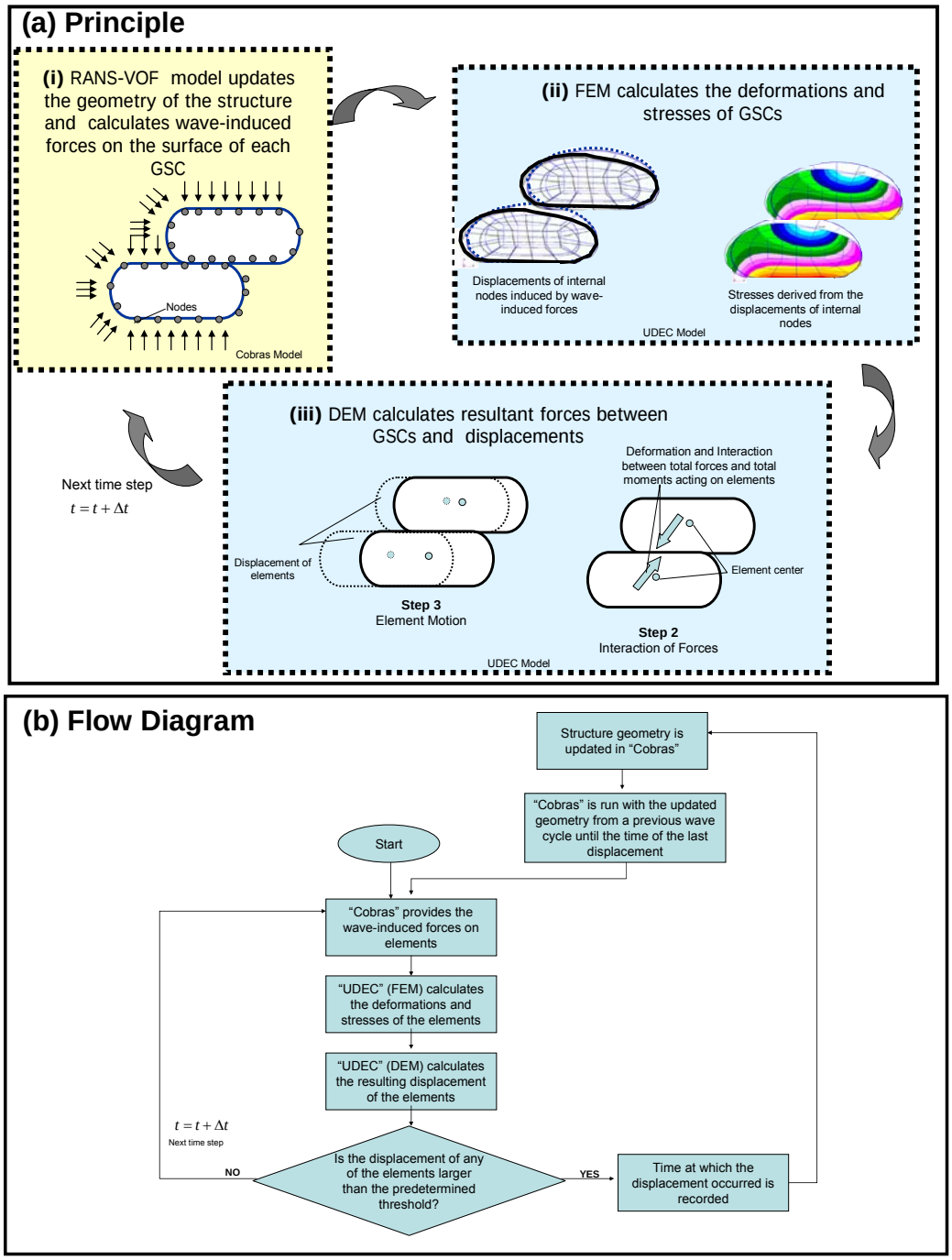

Figure 3: "Partial Coupling" of the Flow and Structural Models

The "partial coupling" of the models is performed as follows (Figure 3):

1) The flow model "Cobras" calculates the wave-induced pressures along the surface of each element (pressures are integrated into forces at each nodal point of the perimeter of the finite element mesh in each GSC, see Figure 3a).
2) The structural dynamic model (FEM in UDEC) calculates the displacements of each node of the GSC (deformations). From the GSC-deformations, the model (FEM) derives the stresses (Figure 3a).
3) From the displacements of the nodes that are in the surface of each element that interact with the neighbouring elements, the structural dynamic model (DEM in UDEC) calculates the resultant forces among each of the GSCs in the structure. The displacement of each element is then calculated by considering the shear properties of the discontinuities and the derived resultant forces (Figure 3a).
4) Finally, the model proceeds to the next time step with an updated geometry (if required).

2.1 Further Details of the Partial Coupling

Since only a "partial coupling" is performed the two main factors that control the accuracy of the simulations are:

(i) **The magnitude of the time step:** Ideally the time step should be as small as practicable, especially for the DEM model. The time step in DEM is critical, since a large time step could induce large indentation between elements and thus, displacement could be unrealistic (see Recio and Oumeraci, 2007b and Itasca, 2004 for more details). On the other hand, a very small time step will increase considerably the computational time. The optimal time step is determined by "trial and error" and depends on the required accuracy of the simulation.

(ii) **Tolerance for updating the structure geometry in "Cobras":** Every deformation or displacement of the elements will disturb the wave-induced flow and thus, the wave-induced forces on the elements in the next time step. With a fully coupled model, the geometry is updated and the subsequent disturbance of the flow considered at every time step. However, with the "partially coupling" as described in Figure 3, updating the geometry of the structure at every time step will not be practicable, so that a more feasible option is to update the geometry of the structure in "Cobras" only after a tolerance has been exceeded (threshold displacement of a GSC higher than a predetermined value) (see Recio and Oumeraci 2007b for details). The value of the threshold for triggering the update in "Cobras" should be as small as computationally possible. A threshold of 5cm ($1/8^{th}$ of the length of the element) showed reliable results. For a preliminary analysis, the threshold can be set very high to speed the computation. Another option is to stop the simulation when the displacement is larger than the threshold. In this case, the results will show where the critical displacement occurred and at which rate. Using this information, it may be predicted, whether the structure will be stable or not.

2.2 Tolerance for Updating the Structure Geometry in "Cobras"

A displacement of any element in a structure subject to wave action will interact with the flow field and will disturb it. This disturbance will affect the wave-induced forces on the structure-elements. Since the flow and structural models are not totally coupled, this interaction between displacements (or deformations) and flow cannot be directly simulated. Another disadvantage is that "Cobras" cannot tackle with moving obstacles. That is, if the geometry of the structure is modified, all boundary conditions (pressure, velocity, acceleration, turbulence) of the elements have to be reset to a previous known condition. If not, the balance is not maintained and the code will collapse. In other words, the geometry of the GSC-structure needs to be updated due to the displacement of the elements according to the following steps (figure 3b):

(i) A threshold displacement should be defined for which the flow is considered disturbed.
(ii) the "coupled models" are run normally until a displacement of any element is larger than the predetermined threshold value.
(iii) the time at which the displacement that is greater than the threshold value is recorded,
(iv) the new geometry (considering the previous displacements) of the GSC-structure is updated in "Cobras"
(v) "Cobras" is run with the modified geometry from a time step smaller than the time at which the displacement occurred (smaller than time recorded in (i); i. e. one wave cycle before the time recorded in (iii).
(vi) "Cobras" simulations runs until the time at which UDEC recorded the displacement (time recorded in (iii).
(vii) from this point, "coupled simulations" continue, and "Cobras" provides the input values for UDEC until another displacement that is higher than the threshold occurs. Then the steps (iii) to (vii) are repeated.

Finally, the "partial coupling" of the models is explained in terms of the programming routines (figure 4).

The "partial coupling" is achieved by sharing files among the two models:

i. While running, "Cobras" will create an ASCII file with wave-induced forces on each node of the "surface" of each element in the GSC-structure for every time step.
ii. UDEC reads its input values from the ASCII file that is being created by "Cobras" at every time step. It is to note that "Cobras" needs to be al least one step ahead of UDEC, "Cobras" has to write the input values before UDEC can read them and since "Cobras" is computationally speaking slower than UDEC. UDEC is started only after several wave cycles of "Cobras" have occurred.
iii. UDEC writes the displacement of every node of the "surface" of each element in an ASCII file (at every time step).
iv. UDEC checks if displacement is higher than the threshold and if "yes", UDEC is "paused" and creates an ASCII file with the updated position of each of the containers.

v. Cobras updates the geometry of the structure by reading the ASCII file that UDEC created with the coordinates of the elements.
vi. "Cobras" is run again with the updated geometry and writes again the wave-induced forces on the ASCII files. When the simulation time in Cobras is equal to the time as the previous displacement threshold occurred in UDEC, UDEC starts again and continues to read the input values from the ASCII file (created by "Cobras") until the next "critical displacement" (displacement higher than threshold) occurs.

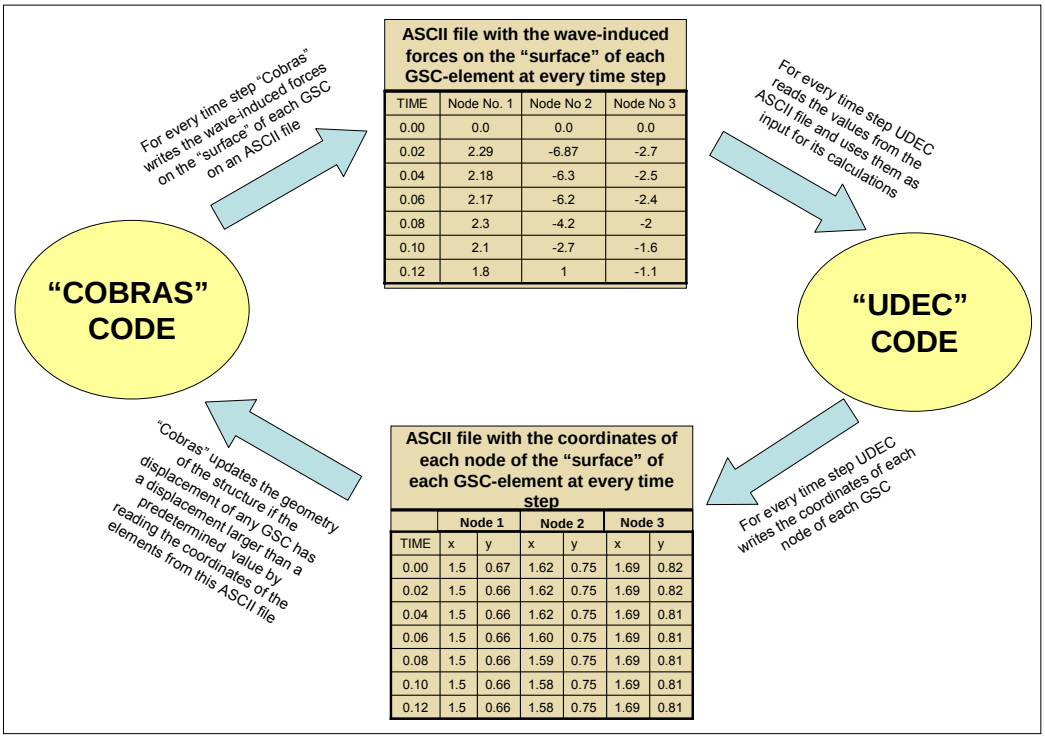

Figure 4: Interchange of Information between the Flow Model ("Cobras") and the Structural Dynamic Model (UDEC).

3. Application of the "Coupled" Model to the Stability of GSC-Structures

The "partially coupled" model is used to simulate the stability of coastal structures made of geotextile sand containers. Recio and Oumeraci (2005a) found that there are many processes that affect the stability of GSC-structures (Figure 5). However, it would be impossible to simulate all the processes that affect the stability of these structures. Regarding the simulation of the GSC, the latter consists of three different areas: (i) the surface of the GSC made of the geotextile, (ii) the interface between the geotextile and the sand and (iii) the sand fill itself (Figure 6). However, one of the limitations of the "coupled" model is that each element needs to be considered as made of a homogeneous material. Therefore some assumptions to change the GSC to a homogeneous material are made (see next section for details).

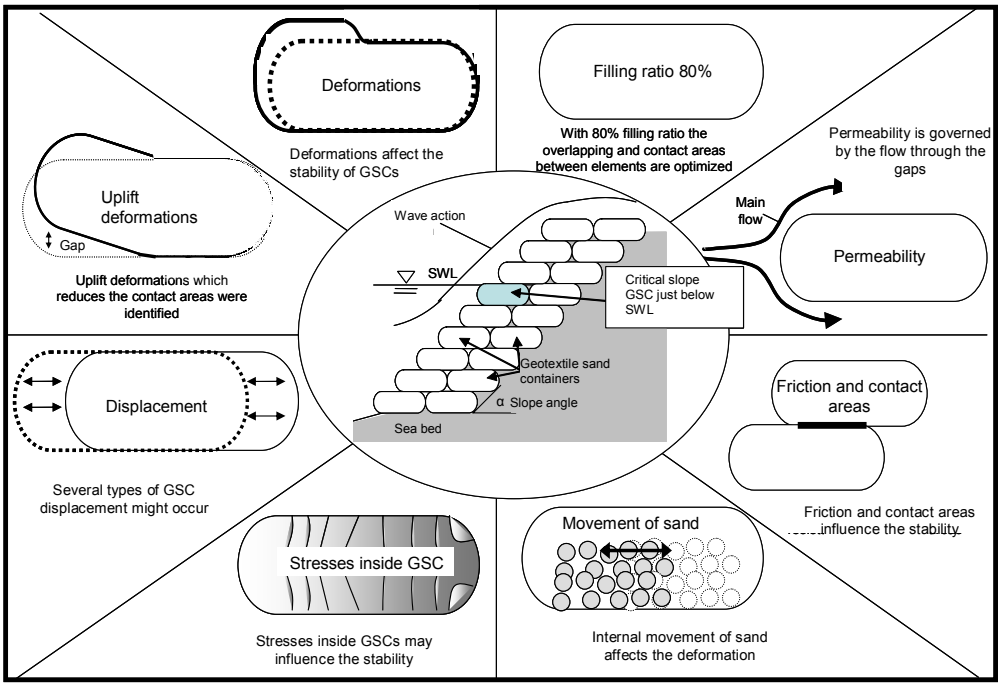

Figure 5: Processes that Affect the Stability of GSC-Structures

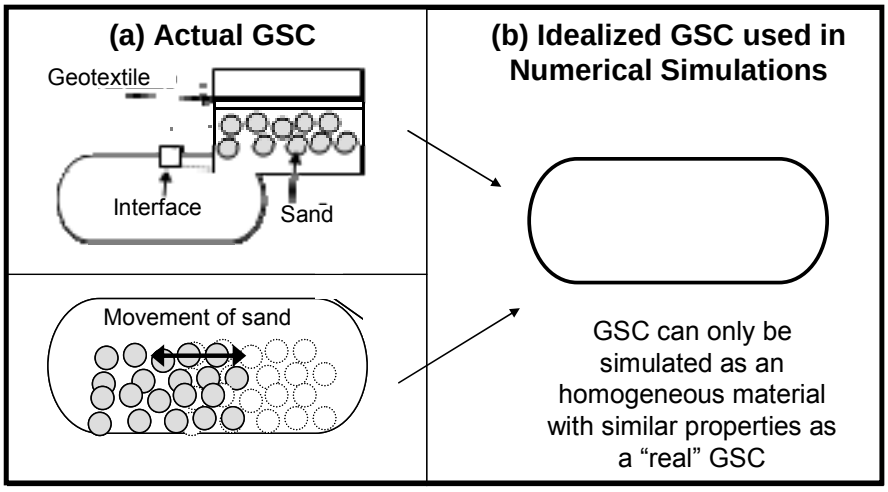

Figure 6: Idealization of a Geotextile Sand Container for Structural Dynamic Computations

3.1 Application of the "Coupled" Model to the Model Tests Performed by Hinz and Oumeraci (2002)

To validate the "coupled" model and to verify its feasibility for simulating the stability of GSC-structures, the "coupled" model was applied to the GSC-structure tested by Hinz and Oumeraci (2002) (Figures 7 and 8). The reasons for choosing these model tests among other available model tests (e.g. Recio and Oumeraci 2006) are:

(i) The size of the GSC-structure tested by Hinz and Oumeraci (2002) is very small compared with the other available tests, thus computational times are smaller.

(ii) Hinz and Oumeraci (2002) performed stability tests and found a stability threshold which depends on the wave conditions (see next section for more details). This stability limit is used for calibrating the threshold between movement and no movement of GSCs in our numerical simulations and then to validate the model.

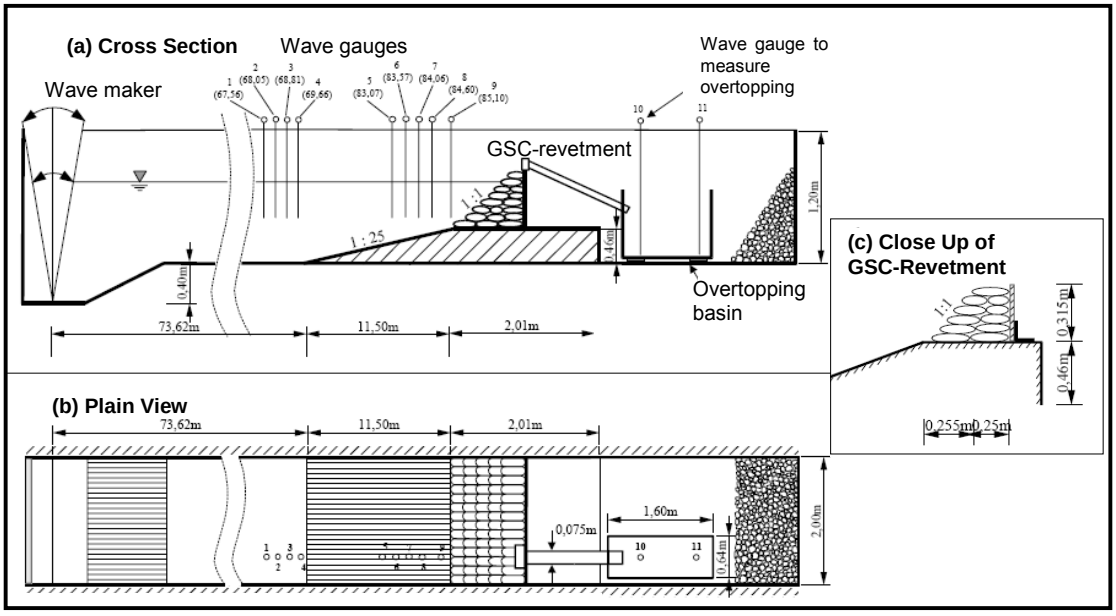

Figure 7: Experimental Set-Up of the Model Tests Performed in the LWI-Wave-Flume by Hinz and Oumeraci (2002)

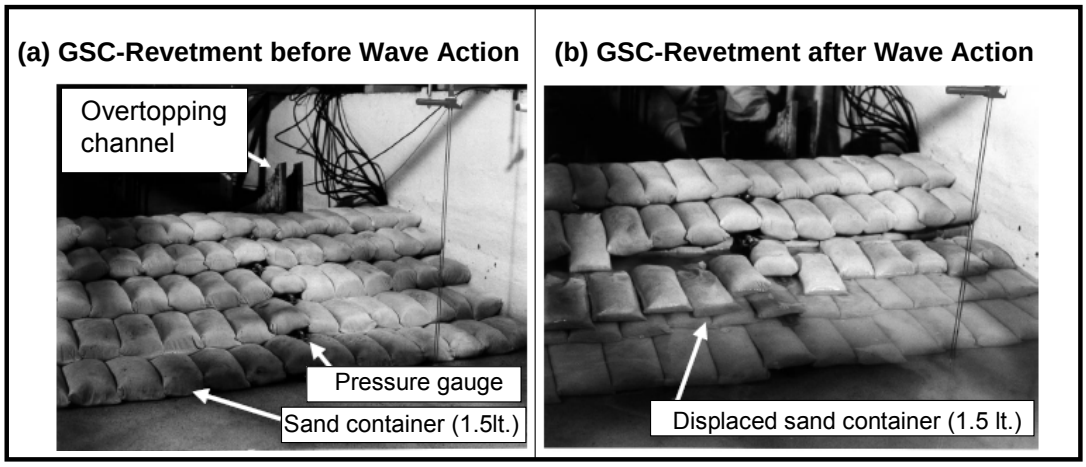

Figure 8: Model Tests Performed in the LWI-Wave-Flume by Hinz and Oumeraci (2002)

3.2 Brief Description of the GSC-Structure and Model Tests Presented by Hinz and Oumeraci (2002)

For these tests a GSC-structure was constructed in the wave flume of LWI using sand filled containers of 0.25 m x 0.1 m x 0.06 m. The slope was 1:1. The structure was subject to different types of regular and irregular waves varying from 0.08 m to 0.20 m with wave periods varying from 1.5 to 4 seconds (Figure 7). Water depth varied from 0.61m to 0.77m.

3.3 Definition of Computational Domain for the Flow and Structural Models

Figure 9 shows the computational domain of "Cobras" in the "coupled" model. In "Cobras", the computational domain consisted in a mesh of 44m long and 1m height with 1200 cells in the horizontal direction and 100 cells in the vertical direction. The mesh was divided in three different zones with different cell sizes. The area near the structure has the smallest grid size consisting in cells of 1 cm x 1 cm. The wave in the flow model is generated using the "internal wave maker" theory. The wave maker is placed approx. 8 meters from the beginning of the left boundary. Waves are of the type "Stokes V". The GSCs in the domain have a 0.25m length and 0.04m height.

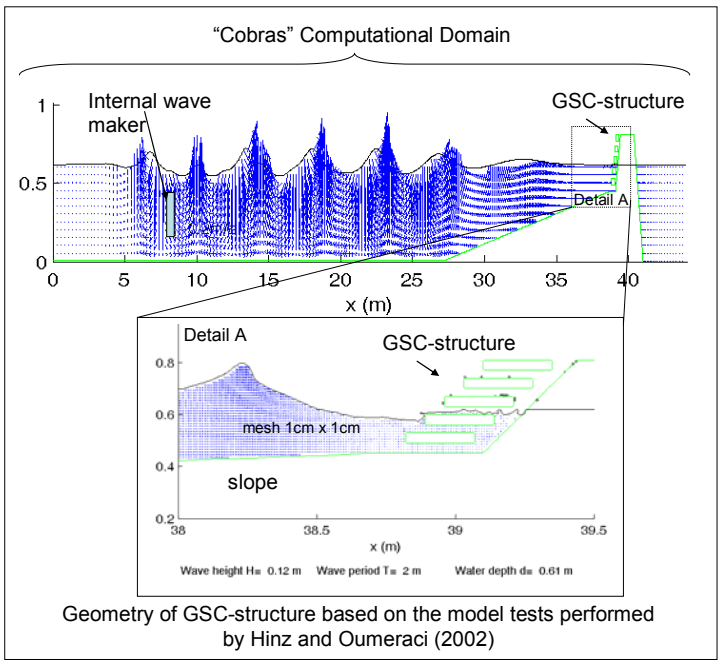

Figure 9: Computational Domain of the Flow Model ("Cobras")

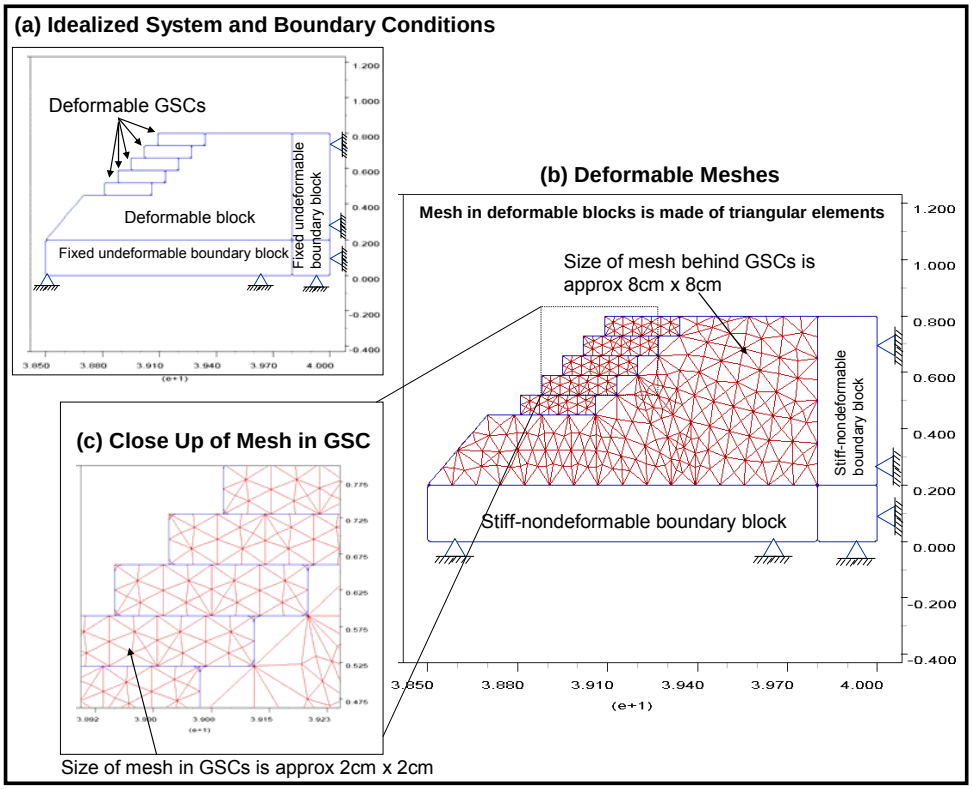

Figure 10: Computational Domain and Discretization in the Structural Dynamic Model ("UDEC")

The computational domain of "UDEC" is shown in Figure 10. The GSC-structure follows the same geometry of the structure tested by Hinz and Oumeraci (2002) with the addition of three fixed blocks at the bottom and right boundaries to make the computational domain stable. The GSC-structure was divided in two different finite triangular meshes: (i) one small mesh for the GSCs (triangular elements in the mesh are approx. 2cm x 2 cm) and (ii) one larger mesh for the rest of the structure (triangular elements in the mesh approx. 8cm x 8cm). As with the flow model, the smaller mesh is implemented in the areas where more accuracy is required (Figure 10). Finally, before the "coupled" simulations the structure was driven to equilibrium by gravitational forces to start the simulations from "realistic" in situ stresses in the structure.

3.4 Additional Considerations for Simulating the GSCs

As mentioned in the introduction of this section, the "coupled" model can only simulate the GSC as homogeneous blocks (internal movement of sand and interface between the geotextile and sand fill cannot be simulated). Therefore the properties of the homogeneous material in the block for the simulations have to be similar to the "average" properties of the GSC.

Matsuoka (2001) performed model tests on the properties of geotextile sand (and other types of soil) containers (see Recio and Oumeraci 2007b and section 2.4). Since it was needed to obtained homogeneous properties for GSCs, the relations obtained by Matsuoka were used for the simulations. Matsuoka found a relation between stress-strain (Figure 11b) of sand bags and "cohesion" values for sand bags which were implemented in the structural model (see Matsuoka 2001 for details).

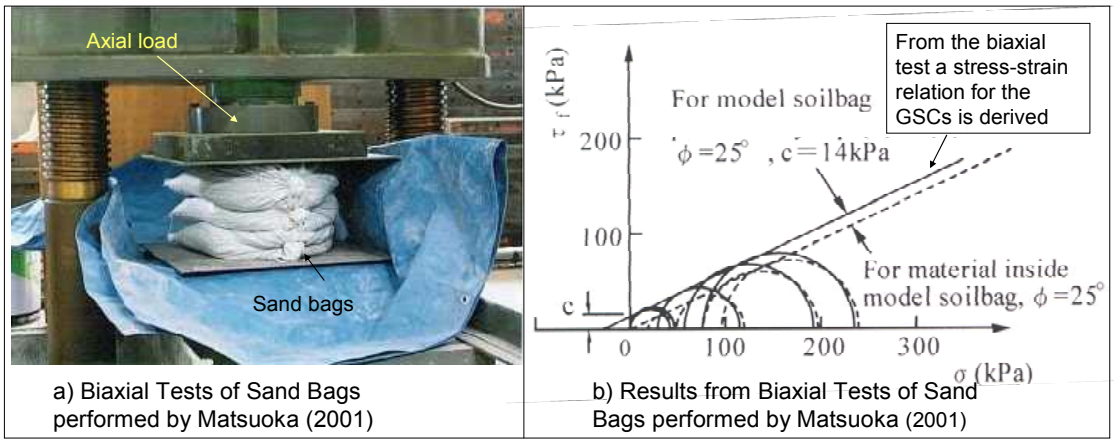

a) Biaxial Tests of Sand Bags performed by Matsuoka (2001)

b) Results from Biaxial Tests of Sand Bags performed by Matsuoka (2001)

Figure 11: Model Tests and Results by Matsuoka (2001)

In addition, Recio and Oumeraci (2005b) and Chapter 4 showed that the internal movement of sand inside a GSC influences the stability of the structure (Figure 12). It was also showed that after the initial wave cycles, an empty area inside the

GSC where the latter "folds" during uprush is formed. Since the internal movement of sand inside the GSC was not simulated, it was assumed that the initial movement (arrangement) of sand inside the GSC has already occurred and that the "folding" area is already formed. This "folding" area is created by reducing the values of the stiffness matrix that correspond to the elements that are in the "folding" area (Figure 12c). For more details on the "stiffness" matrix in FEM refer to Abaqus 2000, Itasca 2004 and Annex 1 of this report.

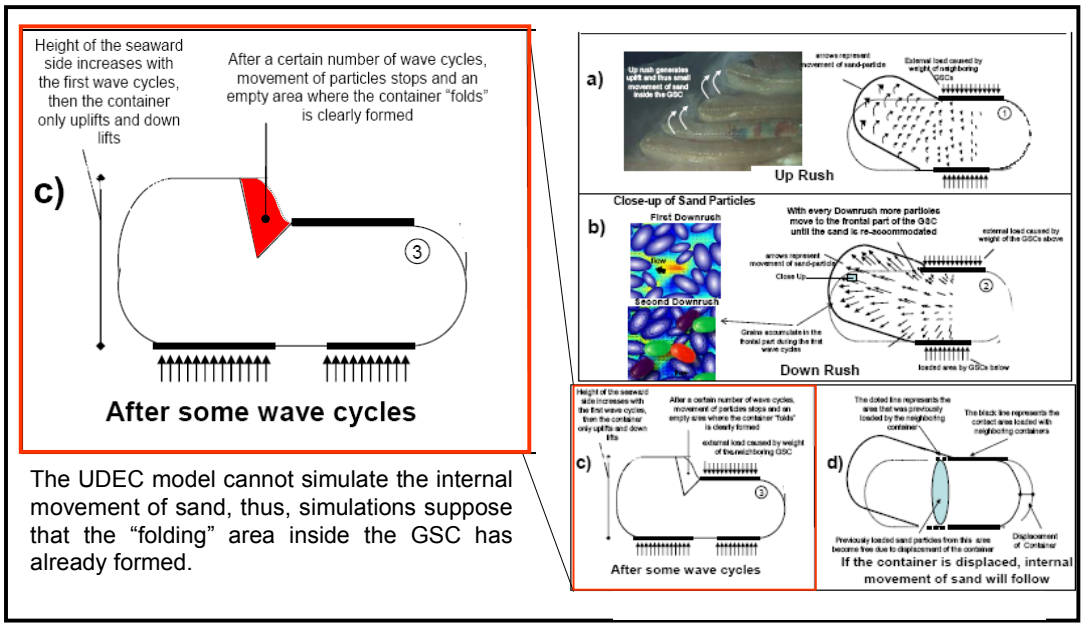

Figure 12: Internal Movement of Sand inside a GSC and "Empty" Area Where the GSC "Folds" During Uprush (Recio and Oumeraci 2006b)

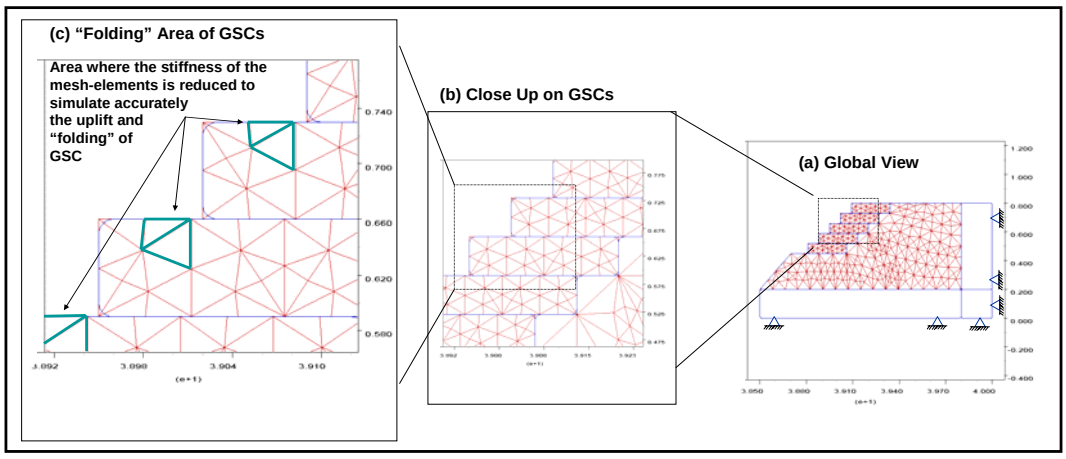

Figure 13: Implementation of the "Folding" Area inside the GSCs in the Numerical Simulation

3.5 Constitutive Model for the Deformation of the GSCs

Seven different constitutive models can be implemented in UDEC. Matsuoka (2001)found from biaxial tests that the behaviour of sand bags is more elastic than the "Mohr-Coulomb" constitutive model. However, in the numerical simulations it was found that the "Mohr-Coulomb" constitutive model agrees better with the deformations observed during the model tests (details on the "Mohr-Coulomb" constitutive model can be found in Itasca 2004 and in most of the Soil Mechanics handbooks). Therefore the Mohr-Coulomb constitutive model was adopted for the simulations.

3.6 Input Parameters for the Numerical Simulations

The main input values used for the "coupled" simulations are summarized in Table 1.

Table 1: Main Input Parameter Used in the Models

"COBRAS" PARAMETERS		"UDEC" PARAMETERS	
Description	**Input Values**	**Description**	**Input Values**
Time step	0.02 s	Time step	0.02 s
Density of water	1000 kg/m^3	Density of all non-submerged deformable GSCs	1800 kg/m^3
Type of wave	Stokes V, Internal wave maker	Density of all submerged deformable GSCs	800 kg/m^3
Kinematic viscosity of water	1x10^{-6} m^2/s	Bulk modulus of GSCs	2.5x10^6 Pa
Turbulence model	$k-\varepsilon$ (nonlinear eddy viscosity)	Shear modulus of GSCs	1.1x10^6 Pa
Turbulence seed parameter	0.5	Cohesion of all GSCs	1.4x10^4 Pa
Eddy viscosity behaviour parameter	5	Bulk modulus of "folding" area inside GSCs	9x10^4 Pa
Max Courant Number	0.3	Shear modulus of "folding" area inside GSCs	4x10^4 Pa
Wave heights	0.08- 0.20m	Friction angle between GSCs	28^o
Wave period	1.5-3 s	Cohesion of "folding" area inside GSCs	1.4x10^4 Pa
Water depth	0.61 m	Maximal displacement of GSC before updating the geometry in "Cobras"	0.05 m
Mesh in domain	1600 x 100	Constitutive model for the deformation of GSCs	Mohr-Coulomb

The values for the fluid dynamic model (Cobras) were selected following the experience from the research team of Professor Philip L F Liu of Cornell University. The values for the structural dynamic model (UDEC) were selected, following the results by Matsuoka (2001) and the values for the "folding" area inside the GSCs were determined iteratively. The friction angle between GSCs was selected, considering the values obtained from large scale shear-box tests performed by Naue (2004) (Table 2).

Using the "partially coupled" model system, several numerical simulations with the same geometry and conditions as tested by Hinz and Oumeraci (2002) were performed. Coupled simulations are shown in the videos attached to this report.

Table 2: Numerical Simulations Performed for Comparison with Experimental Data for a Water Depth of 0.61m.

Wave Height *H* (m)				
Wave Period *T* (s)	0.08	0.12	0.16	0.20
1.5	Num. Sim.	Num. Sim.	Num. Sim.	Num. Sim.
2	Num. Sim.	Num. Sim.	Num. Sim.	Num. Sim.
2.5	Num. Sim.	Num. Sim.	Num. Sim.	
3	Num. Sim.	Num. Sim.		

4. "Coupled" Simulations Results

First, the comparison between the simulated and observed deformation of sand containers and the reduction of contact areas is briefly discussed before embarking into the more quantitative validation with respect to the hydraulic stability.
The comparison of the uplift deformation between experimental data and numerical results is shown in Figure 17 and Table 3. The uplift of the GSC depends on the slope angle of the structure. The differences between experimental and numerical results vary from 29% for uplift deformation of the critical container and to about 12% for the reduction of contact areas during wave action (Figure 14).

Regarding the frontal deformation, it is seen that the numerical model cannot perform in the same way as observed in the model tests, because this deformation is directly induced by the internal movement of sand inside the GSC, which cannot be simulated by the "partially coupled" model Cobras-UDEC (Figure 15).

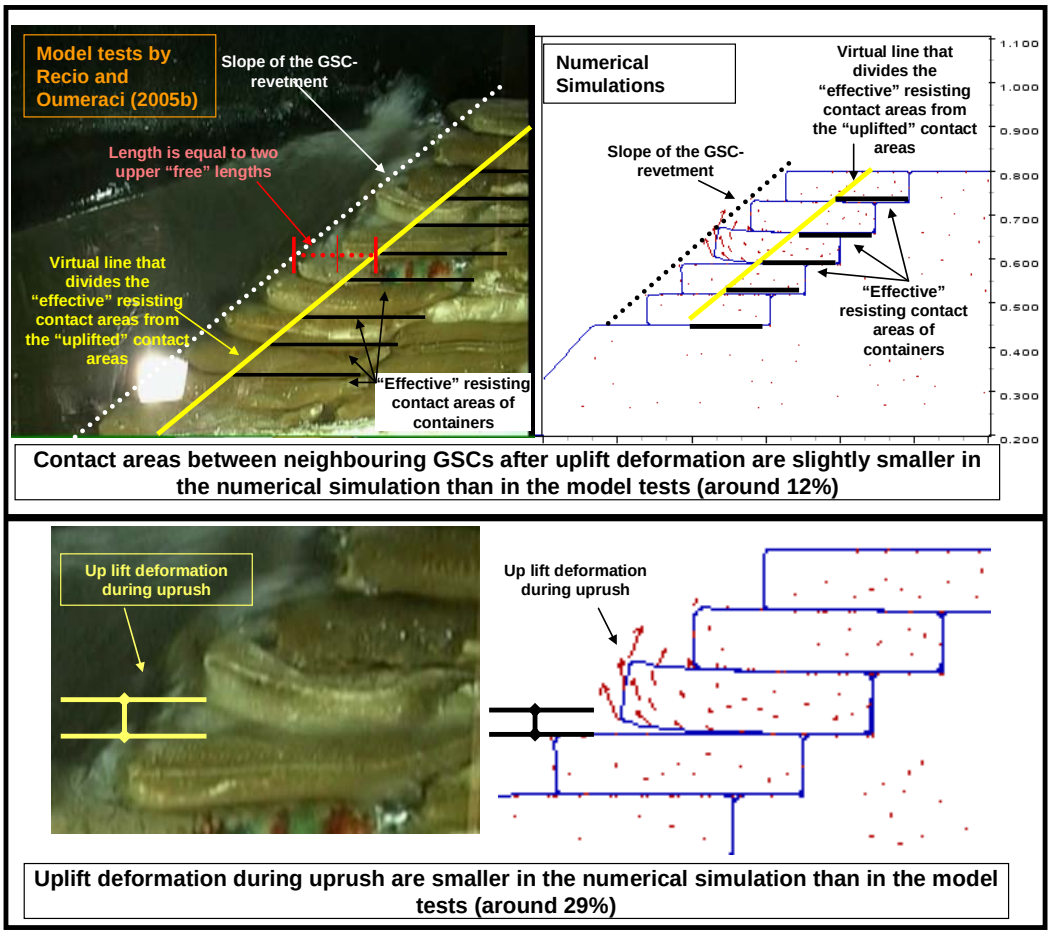

Figure 14: Qualitative Comparison of Computed and Observed Uplift Deformation

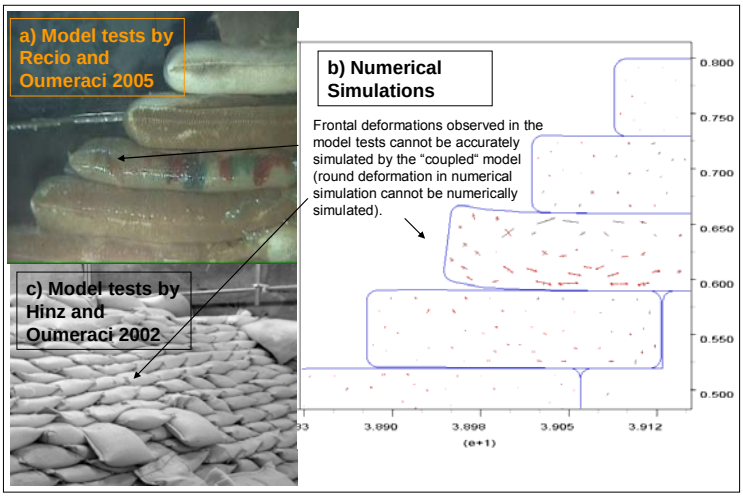

Figure 15: Qualitative Comparison of Frontal Deformation between Numerical and Experimental Results

All numerical simulations were compared with the experimental data obtained by Hinz and Oumeraci (2002). As result of the experiments Hinz and Oumeraci derived stability formulae (Figure 16).

The stability number N_S is plotted as a function of the surf similarity parameter.
For better understand the comparison between experimental and numerical results, the surf similarity parameter (ξ_0) and the stability number (N_S) are described:

$$\xi_0 = \frac{\tan\alpha}{(H_s / L_0)^{1/2}} \qquad (1)$$

where α is the angle of the structure with the seabed, H_S is the significant wave height and L_0 is the wave length in deepwater condition ($L_0 = 1.56T^2$) and,

$$N_s = \frac{H_s}{(\rho_w / \rho_w - 1)D} \qquad (2)$$

where ρ_s and ρ_w are the density of sand and water respectively and D can be expressed as $D = l_c \sin\alpha$; with l_c being the length of the GSC.

The results of the simulations are shown in Figure 17. GSC-structures are stable for a wave height of 0.08m (except the simulation with H=0.08m, T=3s) and for a wave period of 1.5s (except the simulation with H=0.20m, T=1.5s).

Table 3: Numerical Simulation Results of GSC-Structures for a Water Depth of 0.61m

H (m)	T (s)	Ns	Surf Similarity	Stability
0.2	2	1.18	5.59	Unstable
0.2	1.5	1.18	4.19	Unstable
0.16	2.5	0.94	7.81	Unstable
0.16	2	0.94	6.24	Unstable
0.16	1.5	0.94	4.68	Stable
0.12	3	0.71	10.82	Unstable
0.12	2.5	0.71	9.01	Unstable
0.12	2	0.71	7.21	Instable
0.12	1.5	0.71	5.41	Unstable
0.08	3	0.47	13.25	Unstable
0.08	2.5	0.47	11.04	Stable
0.08	2	0.47	8.83	Stable
0.08	1.5	0.47	6.62	Stable

In order to reduce computational time, the GSC-structure was considered unstable, if the displacement of one of the GSCs was observed to increase incrementally with every wave cycle as shown in Figure 18b, where it is clearly seen that the displacement rate within one wave cycle provides information on the stability of the GSC-structure. For example, if the displacement of one GSC is progressive with

every wave cycle, the structure can be considered as unstable. In fact, this assumption is reasonably, since Hinz and Oumeraci (2002) and Recio and Oumeraci (2006) found that the displacement of GSCs is incremental and will continue with every wave cycle until the total detachment of the container from the structure.

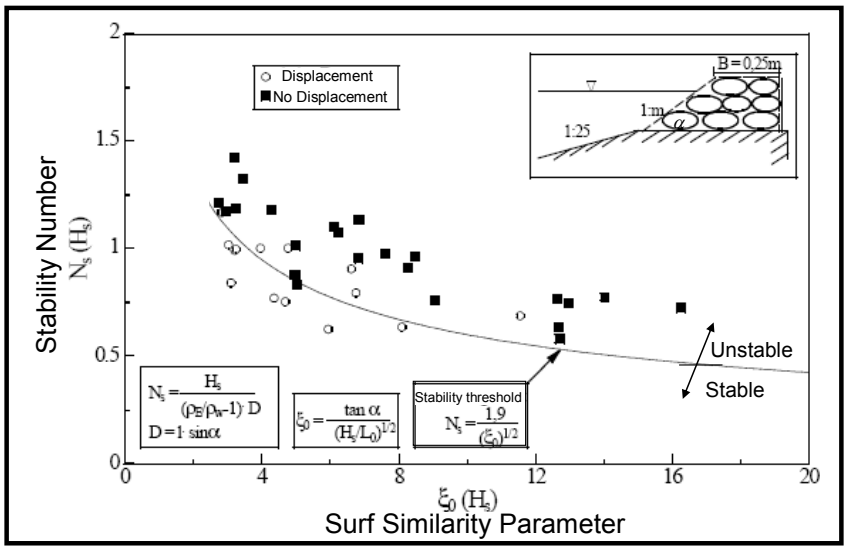

Figure 16: Experimental Results and Stability Threshold for GSCs on the Slope (Hinz and Oumeraci 2002)

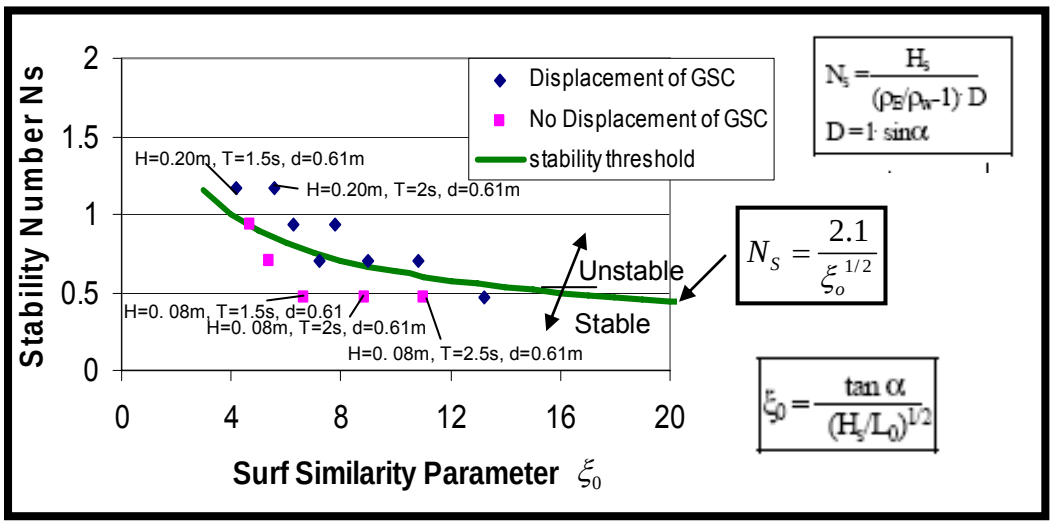

Figure 17: Computed Results for GSCs on the Slope

The stability threshold of the numerical results is plotted and compared with the stability threshold obtained by Hinz and Oumeraci (2002) (Figure 19). The agreement between numerical and experimental results shows qualitative differences as a function of ξ_o of about 10% for the range of $4 < \xi_o < 13$.

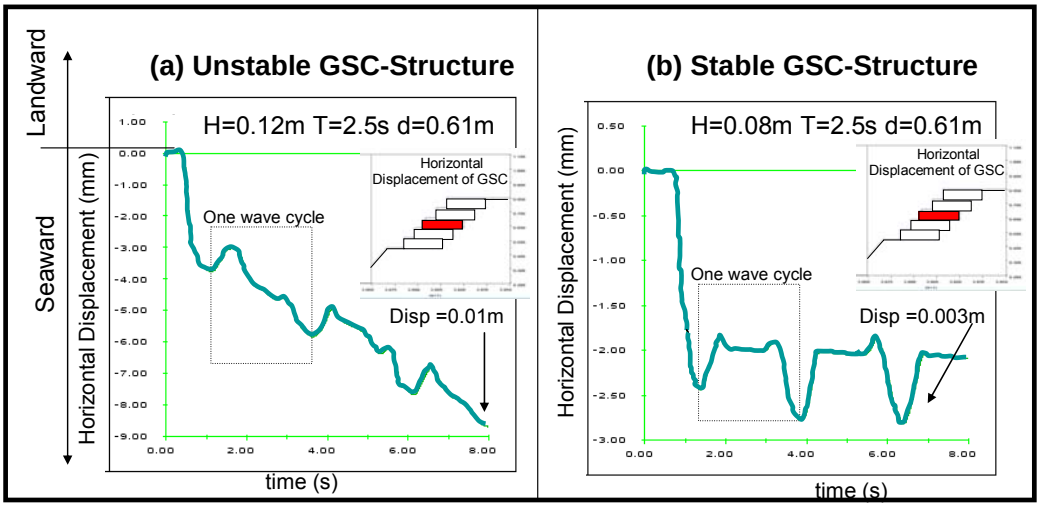

Figure 18: Horizontal Displacement of GSC in a GSC-Structure under Wave Action

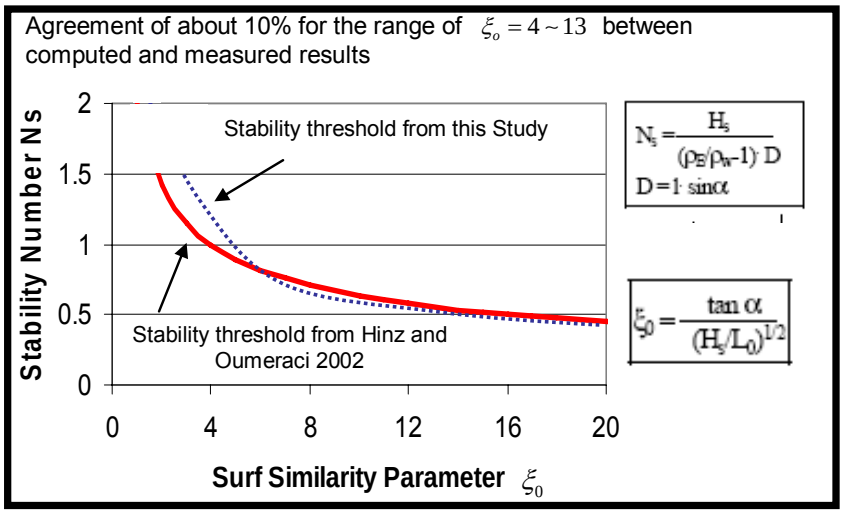

Figure 19: Numerical Results vs. Stability Threshold Derived by Hinz and Oumeraci (2002)

5. Numerical Simulations and Analysis of the Stability of GSC-Structures

Using the validated "Cobras-UDEC" model system, numerical simulations are performed to achieve an improved understanding of the following processes that are associated with the instability of GSC-structures.

5.1 Wave-Induced Deformation on GSCs

The wave induced deformation on GSCs under wave action is shown in Figure 20. The vectors show the displacement of the nodes in the UDEC-model. The container just below still water level suffers the largest uplift deformation. However, as also observed in the model tests, the deformation of other containers, which reduce its contact areas, is also present (see attached videos for more details). There is a qualitatively good agreement with the observed model tests:

(i) The critical GSC is the container located below the still water level (SWL).

(ii) The uplift deformation of the frontal part of the GSC occurs during uprush

(iii) The displacement of the GSC is incremental (stepwise) and occurs mainly during downrush.

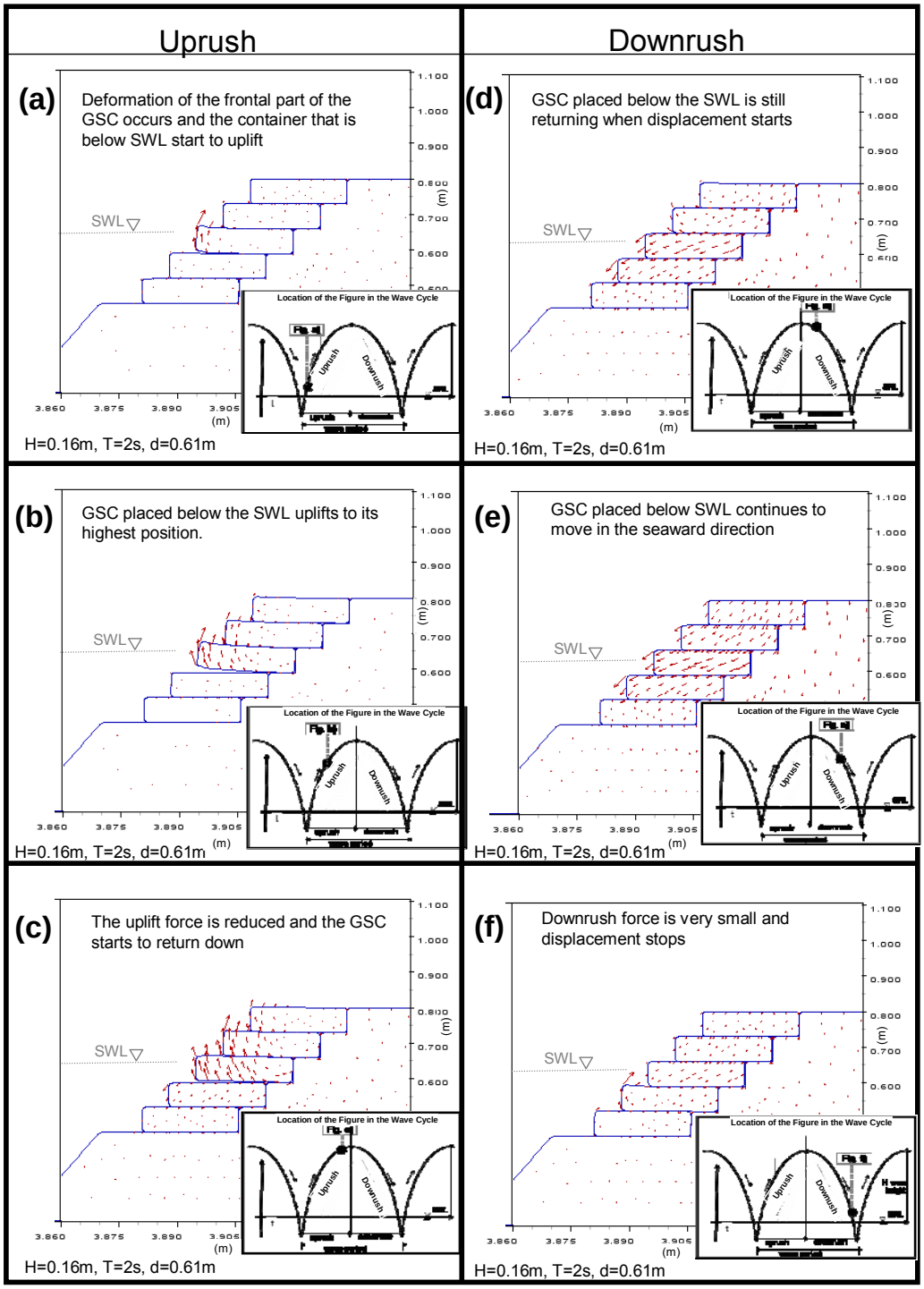

Figure 20: Deformation and Displacements within a Wave Cycle, H=0.16m, T=2s and d=0.61m

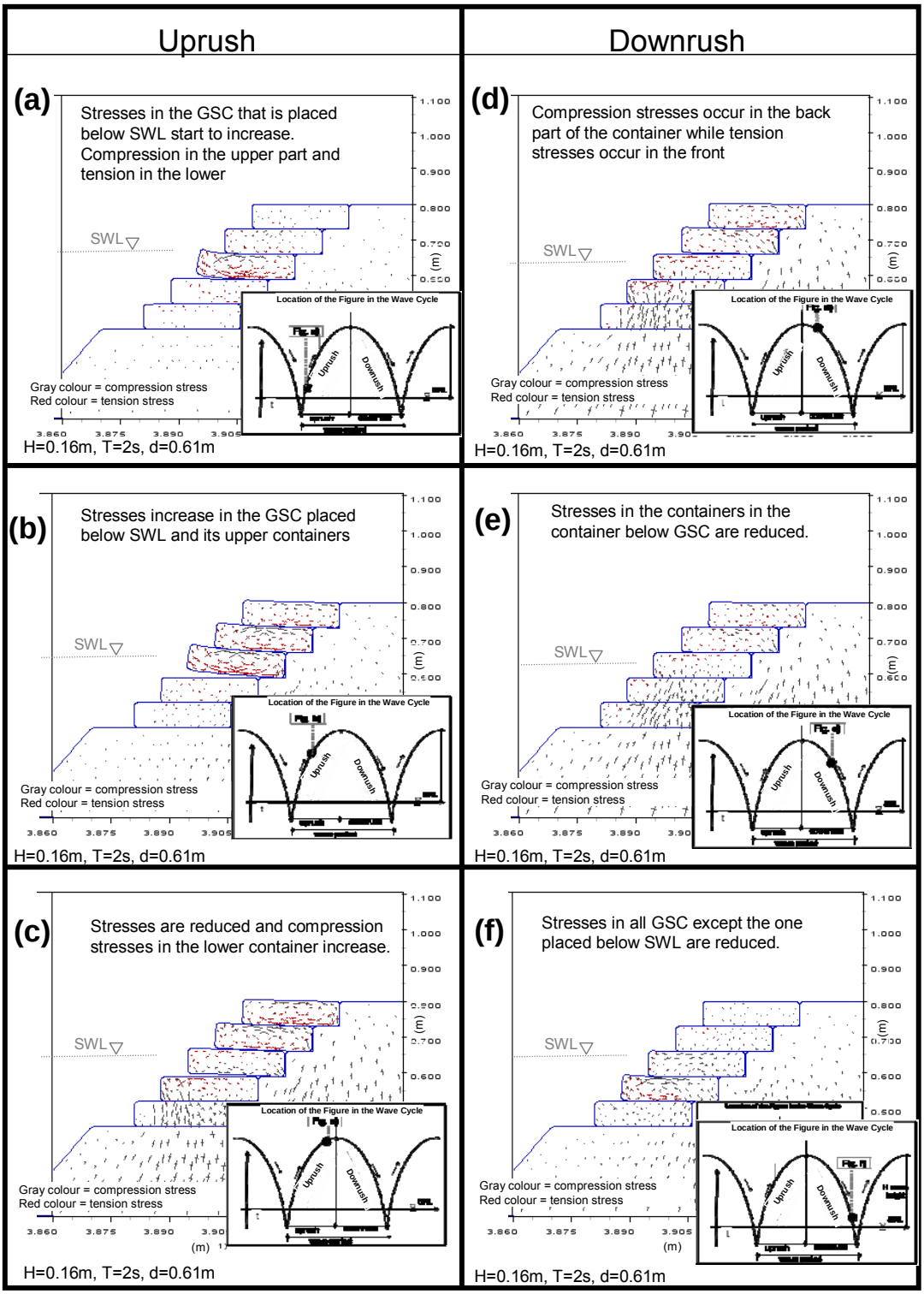

Figure 21: Wave-Induced Stresses within a Wave Cycle, H=0.16m, T=2s and d=0.61m

5.2 Wave-Induced Stresses inside GSCs

The wave-induced stresses on GSC are shown in Figure 21. However, these results need to be treated with caution with respect to the quantitative prediction, since our Cobras-UDEC system cannot simulate the sand inside the container. Nevertheless, they are valuable in the sense that they provide together with the observed results an improved insight into the processes involved. The deformations induce large stresses on the containers.

In addition, at the time when the GSC just below SWL starts to move, stresses are generated at its rear-upper part, showing that even during the displacement of GSCs, the neighbouring GSCs are transferring part of their weight to the GSC underneath, thus, increasing its hydraulic stability.

5.3. Influence of Boundary Conditions on Hydraulic Stability

The boundary conditions influence considerably the stability of GSCs. Comparison of three structures with the same wave conditions but varying in boundary conditions were analyzed by the Cobras-UDEC model system: (i) normal GSC-structure, where critical GSC is just below still water lever with containers above and behind it (Figure 22a), (ii) low-crested GSC-structure with huge overtopping, in which the critical container is subject to restriction in the horizontal axis by the neighbouring container (Figure 22b) and (iii) low-crested GSC-structure, in which the critical GSC has no displacement restriction above or behind Figure 22c).

Numerical results showed that the stability of a container is directly proportional to the number of neighbouring containers that surround it. Numerical simulations showed that the stability threshold and type of displacement depend on the arrangement of neighbouring containers (Figures 22 to 24).
It was re-assured that if a structure is subject to overtopping, the critical containers are those placed at the crest-edge of the structure (Hinz and Oumeraci, 2002).

Crest GSCs consisting in a single layer (cross section) as in Figure 23, are considerably less stable than slope and crest GSCs, which have a neighbouring containers behind (Figure 24).
When a single GSC is subject to overtopping, landward sliding might occur during uprush, while a container with a horizontal restriction will be most probably displaced during downrush (see Figure 24 and attached videos for details).

The most stable containers are those placed on the slope, where the neighbouring containers contribute to the stability (Figure 20).

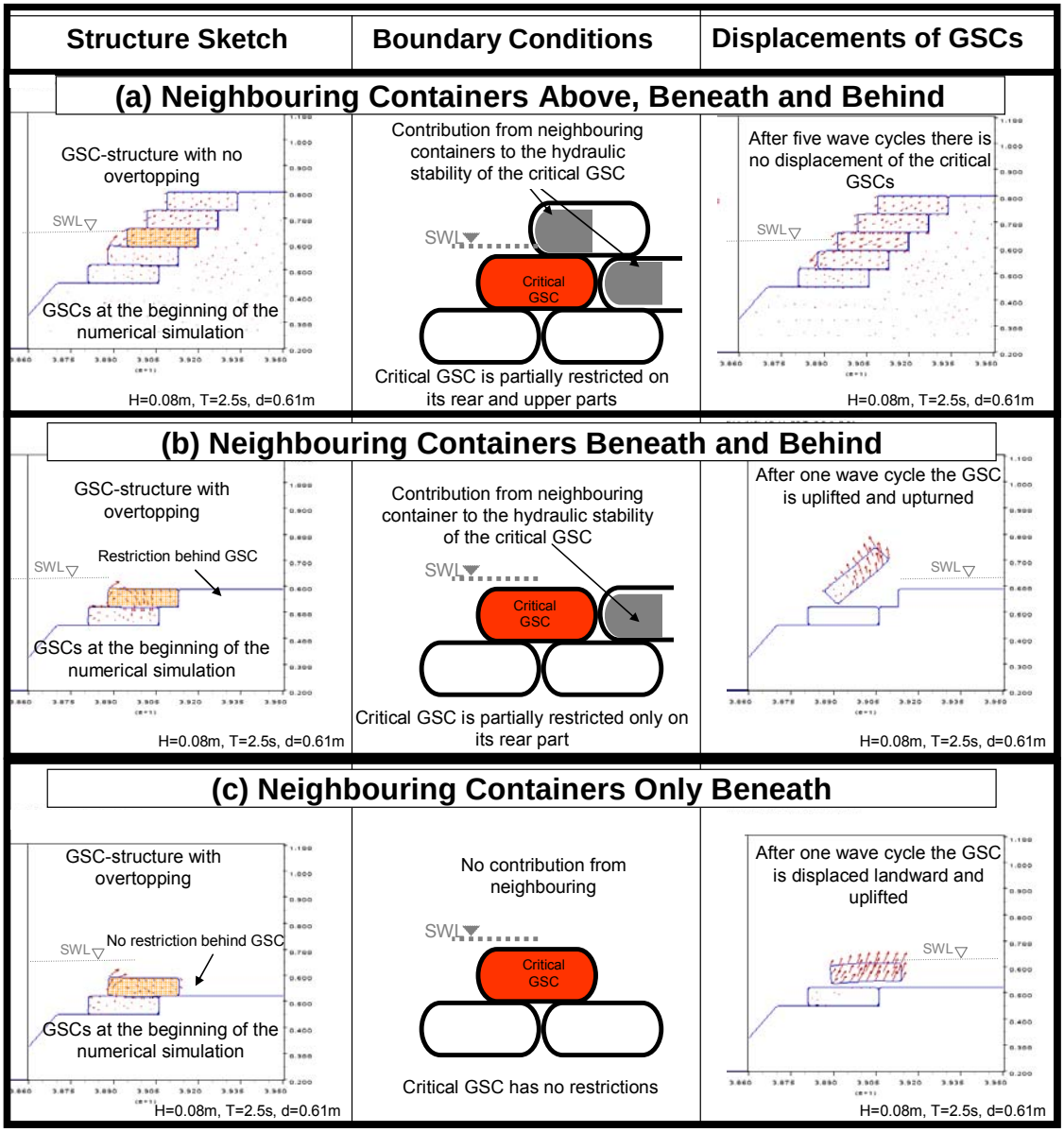

Figure 22: Influence of Neighbouring GSCs on the Hydraulic Stability of GSC-Structures (see also Figures 23 and 24)

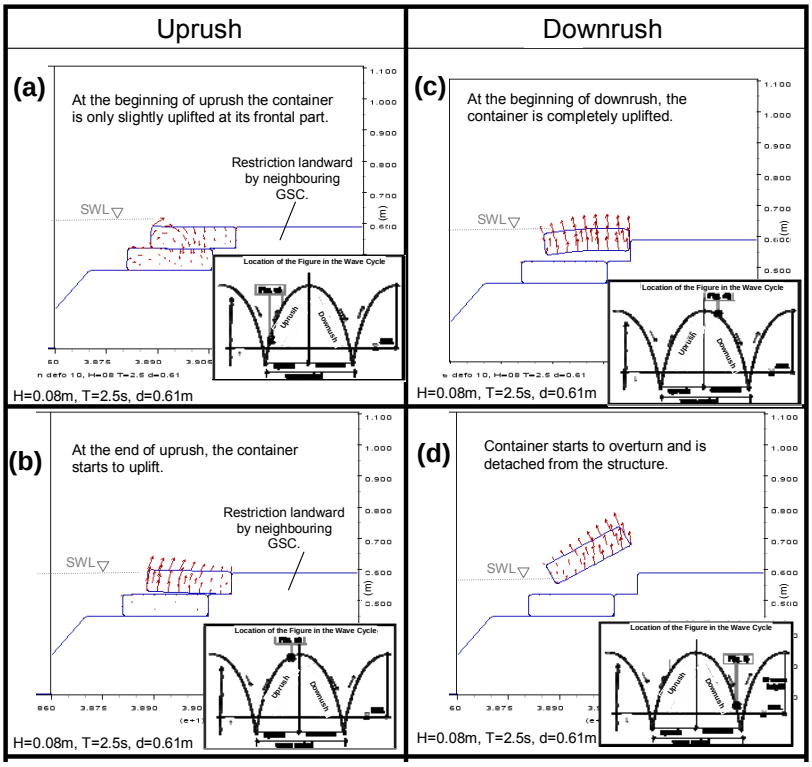

Figure 23: Displacement of Crest GSC with Landward Restrictions

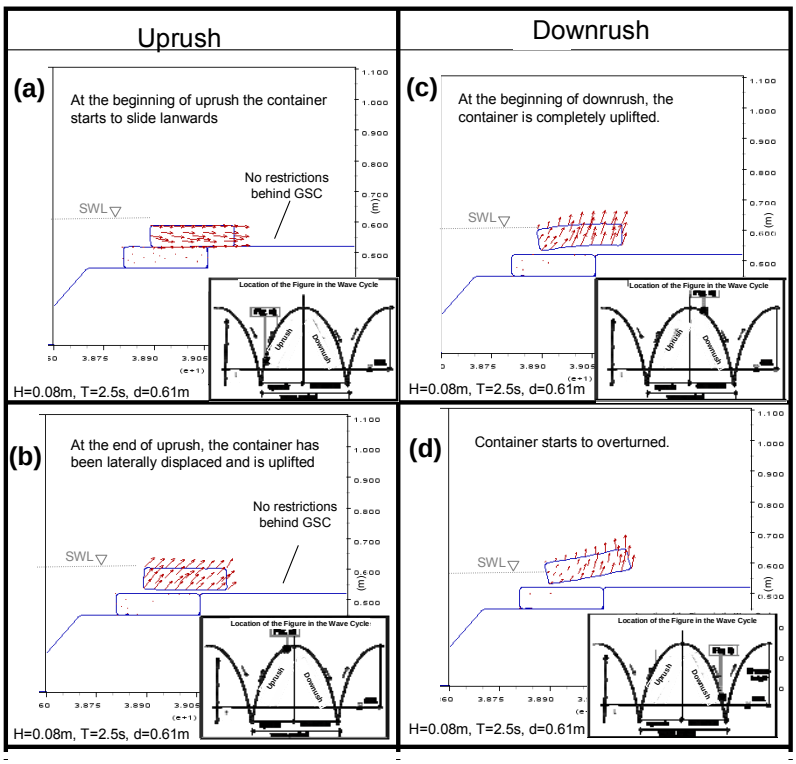

Figure 24: Displacement of Crest GSC with No Restrictions

5.4. Friction between Neighbouring Containers

The "Cobras-UDEC" model system was also used to investigate some relevant parameters that affect the stability of GSC-structures. For instance, the friction between GSCs was found to considerably affect the hydraulic stability.

Consideration of the friction angle between GSCs needs to be considered before deciding the type of geotextile to be used in a prototype GSC-structure. Even a small variation of 10^{o} degrees in the friction angle induces completely different displacements of the GSCs as shown in Figure 25, where a GSC-structure with same geometry and boundary condition but different friction angle resulted in different stability threshold. Therefore, the friction value should be taken from reliable shear stress tests between two geotextiles.

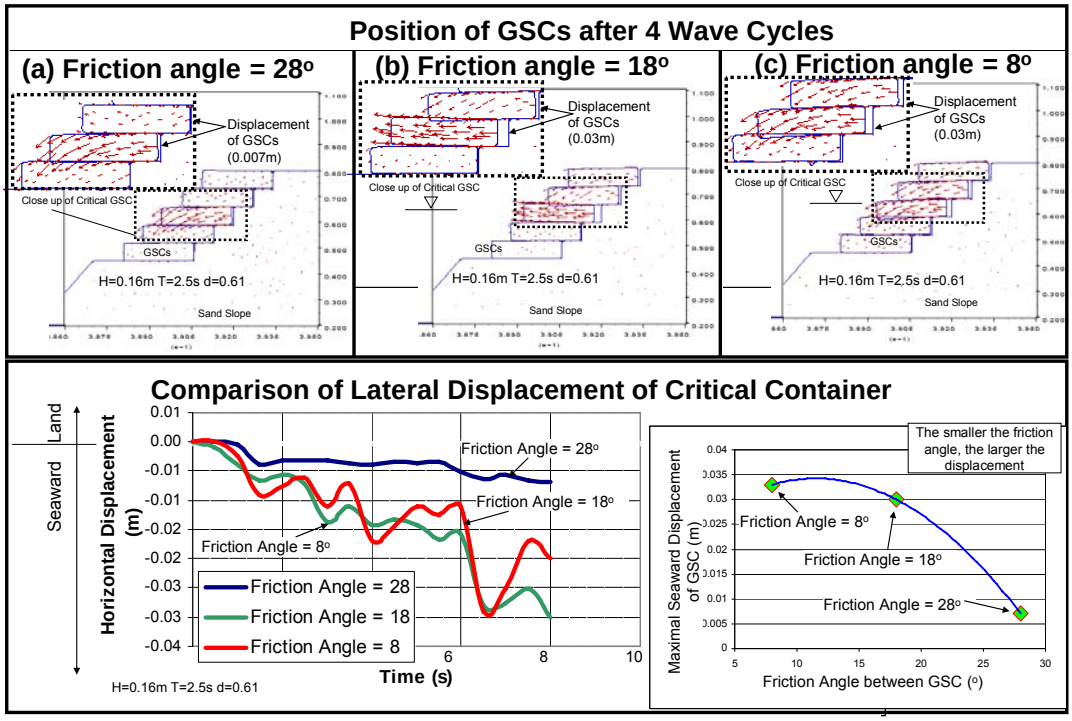

Figure 25: Influence of the Friction Angle between GSCs on the Hydraulic Stability of GSC-Structures (H=0.16m, T=2.5s and d=0.61m)

6. Full Coupling of the Model

Partial "coupled" showed very promising results, however, full and direct coupling of the models is still needed. The direct and total coupling of the models will present several challenges. It is recommended to implement the FEM-DEM model into the flow model ("Cobras"). This due to the fact that the most complex model is the "Cobras" and since the main challenge of the coupling is to implement the flow

disturbance of the flow (flow-structure interaction) due to the displacement of elements.

7. Concluding Remarks

Based on the numerical simulations and analyses presented in this report, the main results can be summarized as follows:

a. The "partially coupled" model system "Cobras-UDEC", used in this study for the simulation of the stability of GSC-structures, has shown surprisingly much better agreement than expected (Stability threshold with variations of 10% for ranges of $4 < \xi_o < 13$).

b. The "partially coupled" model system can however, not describe the internal movement of sand inside the GSC and thus, cannot accurately simulate the frontal deformation of GSCs.

c. The numerical simulations support the conclusion drawn from the experimental results that the critical slope-container on a GSC-structure is the container placed just below still water level.

d. Friction between GSCs considerably affects the stability of GSC-structures and thus, for prototype GSC-structures, it is necessary to better account for this parameter when selecting a geotextile.

e. Numerical simulations showed that the critical areas for the stability of the structure are for the containers placed just below the still water level and at the crest of the structure.

f. By using the here presented "coupled" model the critical areas for the stability, collapse mechanisms and general response of any coastal structure under dynamic load can be investigated. In addition, the coupled model could be used to perform parameter studies of any coastal structure.

g. A coupled RANS-VOF with a FEM-DEM has promising potential as an engineering tool to investigate the stability of coastal structures as well as wave-structure interaction. Any coastal structure could be investigated to identify critical areas for the stability, collapse mechanisms or general response of a coastal structure under dynamic load. However, full coupling of the models is still needed to increase the range of applicability.

6. Annexes

Annex 1: Brief Description of the Finite Element Method
Annex 2: Brief Description of the Distinct Element Method
Annex 3: Potential Use of the "Coupled" Model
Annex 4: Videos of the Numerical Simulations

ACKNOWLEDGEMENTS

The financial support of the author by DAAD and technical advice from NAUE GmbH & Co. KG are gratefully acknowledged.

7. References

Abaqus 2000, Introduction to the Finite Element Method, Hibbitt, Karlsoon & Sorensen, Abaqus Manual, USA

Boutt D, Cook B, Application of a directly coupled numerical model of fluid-solid mechanics, Massachusetts Institute of Technology, 2002. Lecture Notes.

Cundall P.A. 1979. A discrete numerical model for granular assemblies. Geotechnique 29, pag. 47-65

Eberhardt E. 2003., Discontinue Analysis and the Distinct Element Method, Earth and Ocean Sciences at UBC

Grett H. 1984 Das reibungsverhalten von Geotextilien in bindigem und nichtbindigem Boden, Mitteilungen des Franzius-Instituts für Wasserbau und Küsteningenieurwese der Universität Hannover

Harvie D. and Fletcher D, 2000, Volume of fluid advection algorithm, ANZIAM Journal, Australian Mathematical Soc. pp C690-711, Australia.

Hinz M., Bleck M., and Oumeraci H., 2002, Großmaßstabliche Untersuchungen zur Hydraulischen Stabilität geotextiler Sandcontainer unter Wellenbelastun. LWI-Report no. 878. Leichtweiss Intitute, Germany

Itasca Consultants 2004, UDEC Manual, Volume 4, Theory and Background and Volume 1 Users Guide, USA

Kübler; S. 2002, Hydraulische Stabilität von geotextilen Sandcontainern unter Seegangseinwirkung. Diplomarbeit am Leichtweiß-Institut für Wasserbau.

Liu P. 2004, A finite volume/volume of fluid method for solving the navier-stokes-equation with application to water-wave problems, Lecture Notes of the 3 Days Compact Course, LWI, Germany.

Lin P., P.L.-F. Liu, 1998. A numerical study of breaking waves in the surf zone. Journal of Fluid Mechanics 359, 239-264.

Liu, P.L.-F. and P. Lin, 1997. A numerical model for breaking wave: the Volume of Fluid method. Research Report. No. CACR-97-02, Centre for Applied Coastal Research, Ocean Engineering Laboratory, University of Delaware.

Liu, P.L.-F., P. Lin, K.A. Chang and T. Sakakiyama, 1999. Numerical modelling of wave interaction with porous structures. J. Waterway, Port, Coastal and Ocean Engineering, ASCE 125 (6), 322-330.

Matsuoka H., Sihong L. and Yamaguchi K. 2001, Mechanical Properties of Soilbags and their Application to Earth Reinforcement, Proceedings of the International Symposium on Earth Reinforcement, Fukuoka, Japan, 14-16 November 2001 pages 587-592.

Naue, 2004 Direct Shear Stress Results, Internal Communication

Oumeraci, H.; Bleck, M.; Hinz, M.; Kübler, S. 2002b: Großmaßstäbiliche Untersuchungen zur hydraulischen Stabilität geotextiler Sancontainer unter Wellenbelastung. Bericht des Leichtweiß-Instituts Nr. 878, Braunschweig. (in German)

Oumeraci, H.; Bleck, M.; Hinz, M.; Möller, J. 2002a Theoretische Untersuchungen geotextiler Sancontainer im Küstenschutz. Bericht des Leichtweiß-Instituts Nr. 866, Braunschweig (in German)

Oumeraci H.; Hinz, M. 2004, Geotextile sand-filled container as innovative measures for shore protection, Technical paper, Proc. EuroGeo 2004, Vol 1, p. 175-180.

Oumeraci H. Bleck M.. 2001, Hydraulische Wirksamkeit von künstlichen Riffen unter besonderer Berücksichtigung des Energietransfers im Wellenspektrum - Zwischenbericht zum gleichnamigen DFG-Projekt. LWI Bericht Nr. 863.

Pilarczyk Krystian, 1998, Dikes and Revetments, design, maintenance and safety assessment, A.A. Balkema, Rotterdam, the Netherlands

Pilarczyk, K. W. 2000 Geosynthetics and Geosystems in Hydraulic and Coastal Engineering. A.A. Balkema, Rotterdam, ISBN 90 5809 3026, the Netherlands.

Recio J. and Oumeraci H. 2005, Experimental Results obtained from Model Tests, Wave-induced Forces, PIV visualization and Internal Movement of Sand of a Revetment , Progress Report, LWI

Recio J. and Oumeraci H. 2005a, Analyse der Stabilitätsgefährdenden Prozesse von Deckwerken aus Geotextilen Sandcontainer, 5. FZK Kolloquium „Seegang, Küstenschutz und Offshorebauwerke" Hannover, pages 83-87 (in German).

Recio J. and Oumeraci H. 2005b, Experimental Results obtained from Model Tests, Wave-induced Forces, PIV visualization and Internal Movement of Sand of a Revetment made with Geotextile Sand Containers, Leichtweiß Institute for Hydraulic Engineering, Progress Report.

Recio J. and Oumeraci H. 2005c, Effect of the Deformation on the Hydraulic Stability of Revetments made of Geotextile Sand Containers, Proceedings of the International Symposium, "Tsunami Reconstruction with Geosynthetics", Bangkok, Thailand pages 53-68.

Recio J. and Oumeraci H. 2006a, A Numerical Study on the Hydraulic Processes associated with the Instability of GSC-Structures using a VOF-RANS Model, Leichtweiß Institute for Hydraulic Engineering, Progress Report.

Recio J. and Oumeraci H. 2006b, Effect of deformations on the hydraulic stability of coastal structures made of geotextile sand containers. Geotextile and Geomembrane Journal, Elsevier (in print).

Recio J. and Oumeraci H. 2006c, Processes Affecting the Stability of revetments made with geotextile Sand Containers. Proceedings of the International Conference of Coastal Engineering, ICCE 2006, San Diego, USA.

Recio J. and Oumeraci H. 2006d, Geotextile Sand Containers for Coastal Structures, Hydraulic Stability Formula and Tests for Drag, Inertia and Lift Coefficients, Leichtweiß Institute for Hydraulic Engineering, Progress Report.

Recio J. and Oumeraci H. 2007a, "Coupled" Numerical Simulations on the Stability of Coastal Structures made of Geotextile Sand Containers, Leichtweiß Institute for Hydraulic Engineering, Progress Report.

Recio J. and Oumeraci H. 2007b, Enflussfaktoren zur Stabilität von Küstenbauwerke aus geotextilen Sandcontainern, 6. FZK Kolloquium „Küstenschutz und Seebau" Hannover (in print) (in German).

Recio J., 2004. Considerations for Simulating a GSC-revetment using a Numerical Model, Short Progress Report, LWI (internal report).

Recio J., Yasuhara K. and Murakami S. 2001, Model Tests of reinforced sand revetment under assailing ocean waves, Geosynthetics Engineering Journal (Japan) Vol.16, pages 235-243.

Recio J., 2004. Considerations for Simulating a GSC-revetment using a Numerical Model, Short Progress Report, LWI (internal report).

RIPPLE, A computer program for incompressible flows with free surfaces. Los Alamos National Laboratory Report LA-12007-MS.

Schäfer C. 1999, Analysis and Implementation of the Discrete Element Method using a Dedicated Highly Parallel Architecture in reconfigurable Computing

Sitharam T. 2002. Numerical Simulation using Discrete Element Modelling, Research Articles, Current Science, Vol 78, No 7.

Weck O. 2004, Finite Element Method, Massachusetts Institute of Technology (MIT) 2004 Lecture 16.810. USA

ANNEX 1

"Brief Description of the FEM (Finite Element Method)"

1. Introduction

In this annex, a brief description of the Finete Element Method is presented. Detailed information can be found in the references and related-literature. This Annex explains the basis of the FEM, calculation procedure, its advantages and disadvantages.

2. Finite Element Method

FEM is a numerical model to describe mechanical behaviour of continuum structures. FEM was originally created to solve problems of structural mechanics, and it was later applied to many other problems in physics. FEM cuts a structure into several elements and then reconnects elements at "nodes". This process results in a set of simultaneous algebraic equations, which solutions represent the behaviour of the structure.

2.1 Flow of FEM and Calculation Cycle

FEM is a simulation model, this mean that the desire results can vary depending on the problem. Most of researchers use FEM as a tool for obtaining stresses and deformations of continuum structures. Figure 1 shows the flow of a FEM model.

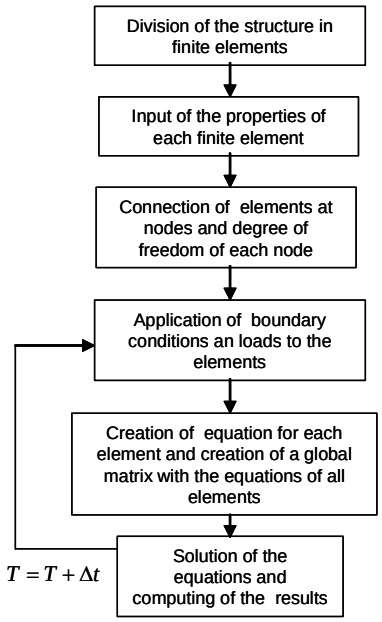

Figure 1 Typical Flow of a FEM Model

The first step in a FEM is to discretize the actual geometry of the structure using a collection of finite elements. Each finite element represents a discrete portion of the physical structure. A simple interpolation function is assumed over the element, representing the shape of the spatial solution in that element. Figure 1 shows and example of the division of a structure into finite elements.

After dividing the structure in elements, it is necessary to assign the connectivity of each element and the degree of freedom of each node. This can be done using especial algorithms. Then, determination of the boundary conditions and loads on

each node of the elements has to be conducted. Free body diagrams for each node can be drawn and solved. In general, each node will carry an external load and internal loads caused by stresses in the elements attached to that node. For the model to be in static equilibrium, the net force acting on each node must be zero, i.e. the internal and external loads at each node must balance between each other.

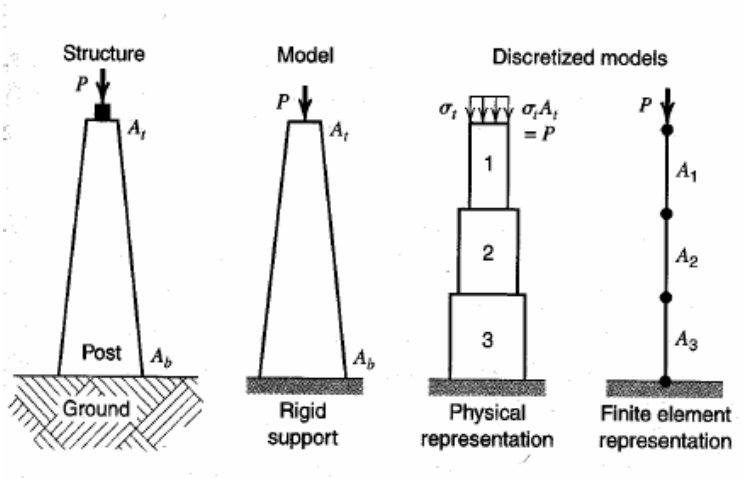

Figure 2: Division of a Structure into Finite Elements (after Weck 1997)

2.2.1 Fundamental Equation of FEM

The basic fundamental of FEM is that instead of obtaining an algebraic equation for the entire domain (which can be extremely complicated), FEM handles algebraic equations for each of the finite elements, and then incorporate all the element equations into a global equation. The basic fundamental equation of FEM can be stated as,

$$[K]\{u\} = \{F\} \qquad (1)$$

where *K* is the matrix representing the element properties, *u* the behaviour of the element and *F* the action. For normal elastic analysis *K* will represent the stiffness*, u* the displacement and *F* the external forces.

The matrix form results from combining the equations for all elements defined in a structure. Thus, [K] is an N x N "property" matrix and represents elements properties (material constants, dimensions, etc.), [u] is an N column vector representing the unknown potential values at each element node. [F] is an N column vector representing the forcing function.

Table 1 shows the most typical uses of an FEM simulation.

Table 1: Basic Simulations in FEM

Simulation Type	*Property [K]*	*Behaviour [u]*	*Action [F]*
Elastic	Stiffness	Displacement	Force
Thermal	Conductivity	Temperature	Heat source
Fluid	Viscosity	Velocity	Body source
Electrostatic	Permittivity	Electric potential	Charge

As all the elements in the structure are connected together through nodes located at their edges, we obtain a system of equations represented in N x N matrices. We only know the values at certain points in the structure (usually at its boundaries). These values are used to get the unknown potential inside the structure. Figure 3 shows how the global equation of the structure can be obtained using FEM.

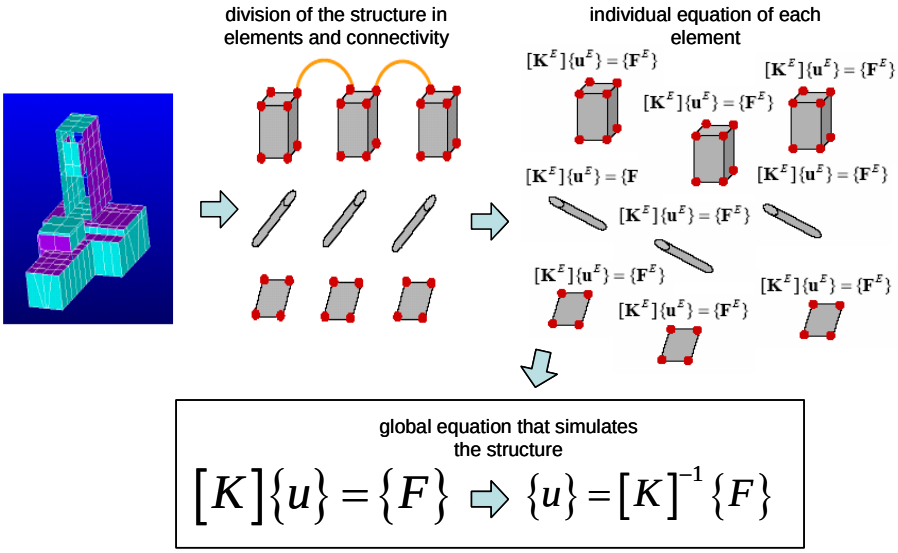

Figure 3: Method for Obtaining the Global Equation in FEM

2.2.2 Solving of Equations in FEM

The equilibrium equations need to be solved simultaneously to obtain behaviours (i.e. displacements, $\{u\} = [K]^{-1}\{F\}$). This requirement is best achieved by matrix techniques.

After the global equations are solved, the final solution would give the distribution of the potential over the structure, represented by the values obtained at the nodes of each element. The precision can be improved by dividing the structure into more elements, or by assuming a more precise distribution of the potential inside the element itself.

After displacements are known, stresses can be easily calculated using elastic-plastic formulae.

The cycle can be repeated for each time step and the results from the global equation at each step will give the simulation of the behaviour of the structure.

2.3 Advantages of FEM

-Can simulate accurately continuum structures

- Can handle bodies comprised of non-homogeneous materials. Every element in the model could be assigned a different set of material properties
- Can handle bodies comprised of non-isotropic materials
- Special material effects are handled (temperature dependent properties, plasticity, creep, swelling)
- Special geometric effects can be modelled

2.5. Disadvantages of FEM

- Cannot handle discontinuities in structures
- A specific numerical result is obtained for a specific problem. A general closed-form solution, which would permit one to examine system response to changes in various parameters, is not produced.

- The FEM is applied to an “approximation” of the mathematical model of a system, results are only approximations which depend on the number of finite elements in the structure.
- Experience and judgment are needed in order to construct a good finite element model.
- A powerful computer and reliable FEM software are essential.
- Certain effects not automatically included (buckling, large deflections and rotations, material nonlinearities, other nonlinearities)

2.6 Flow of FEM in a Geotextile Sand Container

Figure 4 shows the basic flow for simulating a geotextile sand container subjected to external loads.

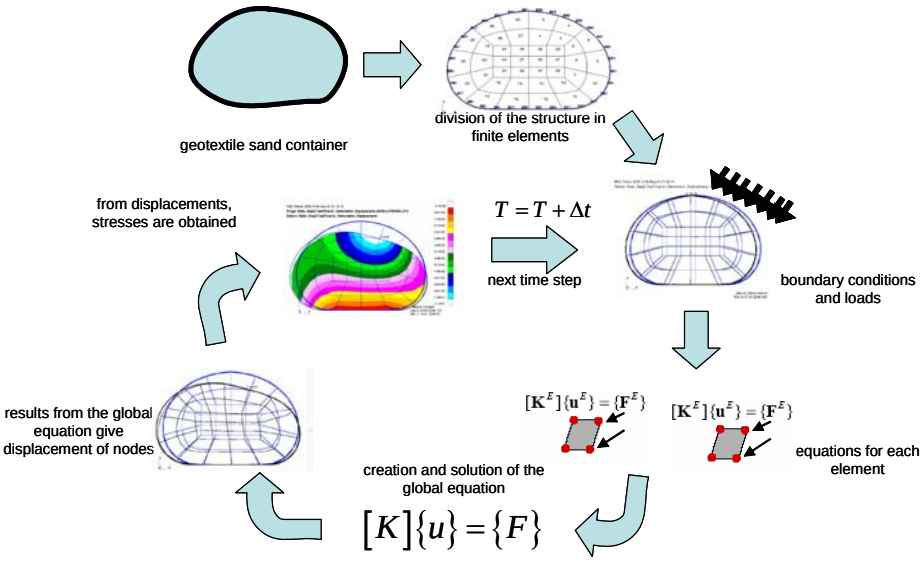

Figure 4: Simulation of a GSC Using a FEM Model

References

Abaqus,2000, Introduction to the Finite Element Method, 2000, Hibbitt, Karlsoon & Sorensen, Inc. USA

Saadawi H.1997, Improving the Finite Element Method using Cell-DEVS, Dept. of Systems and Computer Engineering, Carleton University, USA

Weck O. 1997 Finite Element Method, Massachusetts Institute of Technology (MIT) 2004 Lecture 16.810. USA

Recio and Oumeraci 2004, Feasibility of Using FEM for simulating GSC-structures, Short Progress report. LWI.

ANNEX 2

"Brief Description of the DEM (Discrete Element Method)"

1. Introduction

In this annex, a brief description of Discrete Element Method is presented. Detailed information can be found in the references and related-literature. This Annex explains the basis of the DEM, calculation procedure, its advantages and disadvantages.

2. Discrete Element Method

DEM is a numerical technique pioneered by Cundall (1979) for mechanic problems where the continuity between elements does not exist.

The discrete element method is a numerical model to describe the mechanical behaviour of discontinuous structures. DEM treat structures as an assemblage of distinct interacting elements or bodies that are subjected to external loads and are expected to suffer large displacements. DEM utilizes a calculation procedure that solves the equations of motion and contact force for each of the elements. The basis is that the dynamic equation of equilibrium for each element is formulated and repeatedly solved until the boundary conditions and laws of contact and motion are satisfied.

In DEM, the equilibrium contact forces and displacements of an assembly of elements are found through the medium of disturbances originating at the boundaries, which is a dynamic process. The speed of propagation is a function of physical properties of the discrete medium. DEM is based on the idea that this time-step may be chosen so small that during a single time step disturbances cannot propagate from any element further than its immediate neighbours. This is the key feature of DEM which makes it possible to model the interaction of large number of elements. One of the important features of the DEM model is the explicit incorporation of Coulomb's frictional behaviour at contacts between elements. Slippage between elements is permitted, when the tangential or shear force at a contact exceeds a critical value, defined by:

$$F_s^{\max} = c + \tan\phi \cdot F_n \qquad (1)$$

where F_n is the normal force at the contact, and c and ϕ are the cohesion and the angle of internal friction at contacts, respectively.

2.1 Flow of DEM and Calculation Cycle

A basic flow chart for the DEM is shown in Figure 1. The method is based on the assumption that elements only exert forces on one another when they are in contact. A simulation starts by assuming some initial configuration of the elements, and then calculating which of the elements are touching. The simulation then proceeds by stepping in time, applying the sequence of operations of Figure 1 at each step. The force between two particles can be calculated from the strength of the contact between them. The resultant force on a element is the vector sum of the forces exerted by each of its neighbours. Once the resultant force on each element has

been computed, it is simple to compute a velocity and position increment for each element. Finally, the list of which elements are in contact must be re-calculated.

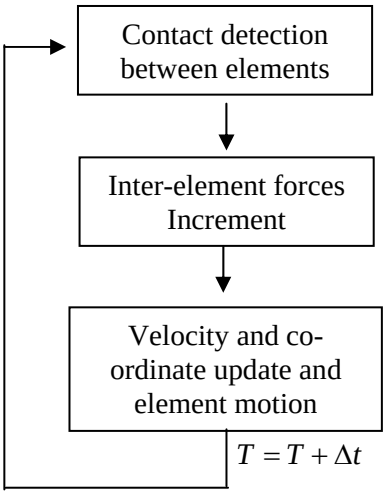

Figure 1 Flow Chart for Calculations Performed in the DEM

2.1.1 Contact Processing and Detection

The essence of contact detection is the determination of the surfaces and volumes of intersection between two elements. Once the contact geometry has been determined, one can easily enforce the contact conditions. This is done through a contact algorithm which checks every face/point contact of every element with every face/point of every other element. For each element, a "contact list" is formed, which contains references to each of the element with which it makes contact.
Supposing two circular elements, contact could be determined from the following equation,

$$\Delta n = R_1 + R_2 - \sqrt{(x_1 - x_2)^2 + (y_1 + y_2)^2} > 0 \qquad (2)$$

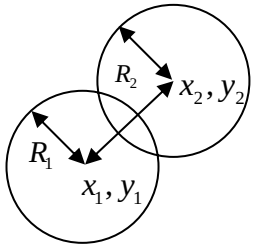

Figure 2: Elements in Contact

where x_i y_i are the co-ordinates of each element's centre and R_1 and R_2 are the respective radius. Δn is the degree of overlap of the elements; the repulsive force between elements is proportional to this overlap. If the condition of equation 2 is true, the addresses of the two elements are added to each others' adjacency list. Contact information can be represented by a simple data structure, in which each element has memory slots allocated to hold the identities of the elements in contact. For non-circular elements modifications to equation 2 are necessary.

2.1.2 Interaction and Inter-Element Forces

Once the contact list for a element has been established the total force acting on it can be determined. This will require a full solution of equation 2 for each contact point identified.

For every contact identified between two elements, the resulting force is calculated. Considering two circular elements, a simple force-displacement law can be adopted therefore the resulting force between two elements is proportional to the indentation between them:

$$F_{xi} = k_n \Delta n_{xi} \quad (3)$$

$$F_{yi} = k_s \Delta n_{yi} \quad (4)$$

$$M = F_s R \quad (5)$$

where k_i is the stiffness (normal and shear), Δn_i is the elements' indentation, given by equation 1, M is the moment, and R is the radius of the elements. The resultant force on a element is the vector sum of the forces caused by each contact with its neighbours.

$$F_x = \sum_i F_{xi} \quad (6)$$

$$F_y = \sum_i F_{yi} \quad (7)$$

$$M = \sum_i F_i R \quad (8)$$

2.1.3 Element Motion

Once the resultant force on each element has been calculated, these forces are used to find new accelerations using Newton's second law:

$$a_x = F_x / m \quad (9)$$

$$a_y = F_y / m \quad (10)$$

Supposing that all elements have identical masses. These accelerations are integrated to obtain the velocities in the x and y direction and the angular velocity

$$v_x = v_{x0} + a_x \Delta t \quad (11)$$

$$v_y = v_{y0} + a_y \Delta t \quad (12)$$

$$\theta' = \theta' + \frac{M}{I} \Delta t \quad (13)$$

As is usual for time integration schemes, the time step has to be small enough that no disturbance can travel beyond one contact in one time step. The new coordinates can be found adding the original coordinates with the incremental displacement obtained by integrating the obtained velocities:

$$x = x_0 + v_x \Delta t \quad (14)$$

$$y = y_0 + y_x \Delta t \quad (15)$$

$$\theta = \theta + \theta' \Delta t \quad (16)$$

2.2 Damping of Elements

DEM includes two forms of damping such as contact damping and global damping. Contact damping (C_n) operates on relative velocities at the contacts and is visualized as resulting from dashpots acting at normal and shear directions at the contact as shown in Figure 3. The contact damping coefficients are taken to be proportional to contact stiffness.

Global damping (C_m and C_1) operates on the absolute velocities and is visualized as the effect of dashpots connecting each element to the ground. Coefficients of global damping are taken proportional to absolute velocities of both translational (C_m) and rotational movement (C_1). Friction damping (C_s) occurs during sliding when the absolute value of the shear force at each contact is at the value of $F_s^{\max}$. The use of additional damping other than friction is necessary in order that the assemblies reach a state of equilibrium for all conditions. If neither contact nor global damping were included, the assemblies could only reach equilibrium if slip occurred. Detailed information on damping and friction calculations can be found in Eberhardt (2003).

k_s	Normal stiffness
k_n	Shear stiffness
I_A	Inertia of element A
m_A	Mass of element A
C	Damping coefficients

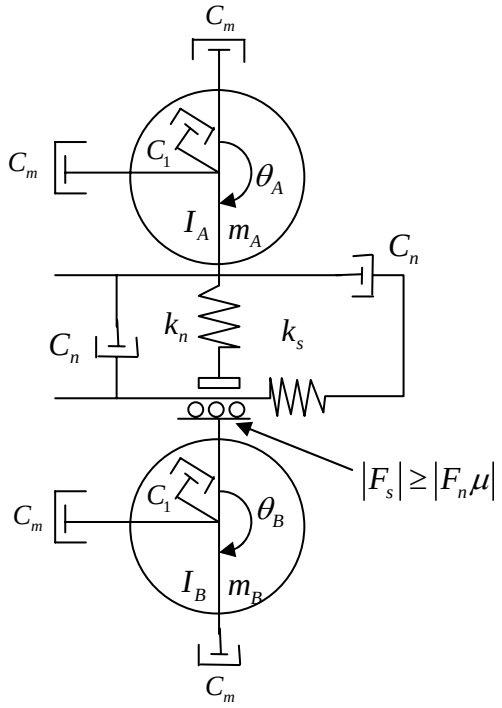

Figure 3: Elements of DEM along with the Damping Mechanism Adopted in DEM

2.3 Flow of DEM in a GSC-Structure

Figure 4 shows the basic DEM-flow of two geotextile sand-containers. For GSCs, DEM can simulated simultaneaously many elements. For clarity purposes only two are shown in Figure 4.

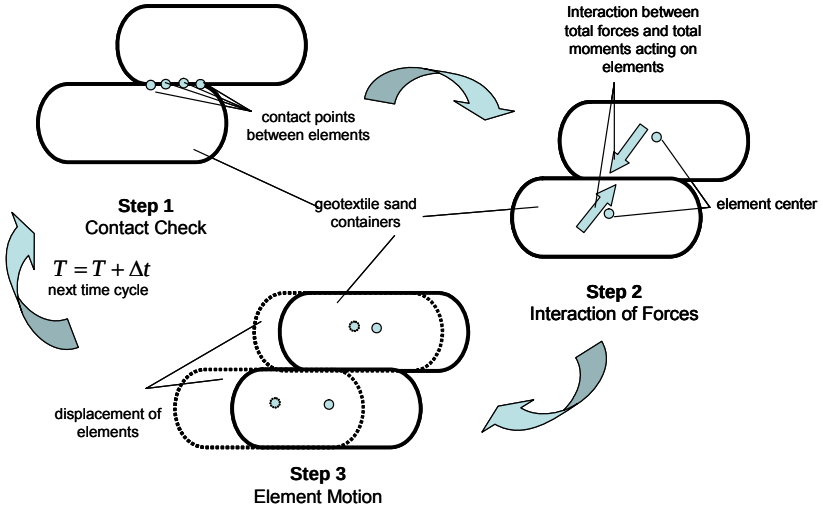

Figure 4: Basic Modelling Steps for Geotextile Sand-Containers using DEM

2.4 Advantages of DEM

- Simulates accurately discontinuous mediums
-Allows movement of elements relative to each other
- Can simulate complex geometries
-Simulates simultaneously slip, rotation and displacement of many elements
- Is an useful tool in understanding the physics of the processes and problems in discontinue mediums
- DEM clearly simulates deformation mechanisms in jointed and particulate media in a more realistic way than any of the continuum-based models

2.5. Disadvantages

- Computational expensive, many time steps are necessary for each simulation.

References

Cundall P.A. et at., 1979. A discrete numerical model for granular assemblies. Geotechnique 29, pag. 47-65

Eberhardt E. 2003, Discontinue Analysis and the Distinct Element Method, Earth and Ocean Sciences at UBC

Schäfer C. et al, 2000, Analysis and Implementation of the Discrete Element Method using a Dedicated Highly Parallel Architecture in reconfigurable Computing

Sitharam T. Numerical Simulation using Discrete Element Modelling, 2000, Research Articles, Current Science, Vol 78, No 7.

ANNEX 3

"Potential Use of the "Coupled" Model and Future Work"

In this annex, the potentiality of using UDEC for simulating coastal structures is presented.
Since the time frame of this study is limited, it was decided not to directly couple the flow and structural dynamic models. However, even this "partially" coupled model can be used for analyses of coastal structures under wave action.
The approach presented in this study (flow model coupled with a FEM-DEM model) has a great potential for analyzing coastal structures. As an example of the potentiality of the "coupled" model, a numerical simulation of a fictitious breakwater was performed.
A Caisson breakwater placed on a rubble foundation is shown in Figure 1. The caisson dimensions are 1.5m x 1.5 m, the rubble foundation has a layer thickness of 0.70m and the D_{50} of the rubble mound is 0.30 m. The density of the caisson and the rubble is 2000 kg/m^3. The friction angle between the rocks was decided to be small (10^o) to induce displacement and to make the simulation interesting. The whole structure was subject to the following wave conditions: water depth d= 1.2m, T=3s, H=1.0 m. The rubble mound blocks located behind the caisson breakwater were fixed (no allowable displacement), to increase computational velocity. Thus, the objective of the simulation is to investigate the response of the caisson and frontal part of rubble mound under wave action.
Figure 25 shows the result of the simulations. The wave induced forces on the caisson are smaller than the resistant force of the caisson. The interesting part occurs in the frontal part of the rubble mound. With every wave cycle there is displacement seawards of most of the elements (Figure 2). The results of the simulation show that the caisson is well design but that the rubble mound is instable under these conditions (probably due to the slow friction between them).
This example illustrates the potential of the "coupled" model to perform parameter studies or the usage of the "coupled" model as tool during preliminary design stages. By using the "coupled" model, any coastal structure could be investigated to find out critical areas for the stability, collapse mechanisms or general response of a coastal structure under dynamic load.

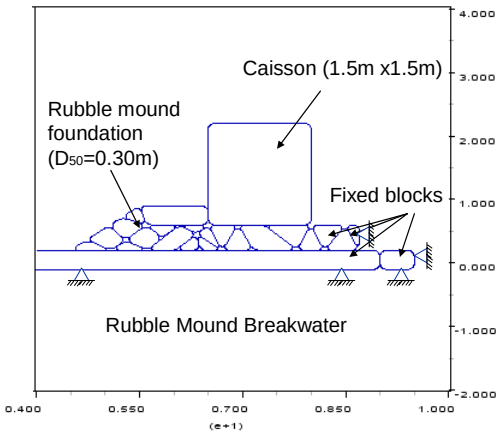

Figure 1: Computational Domain of a Caisson breakwater under Wave Action

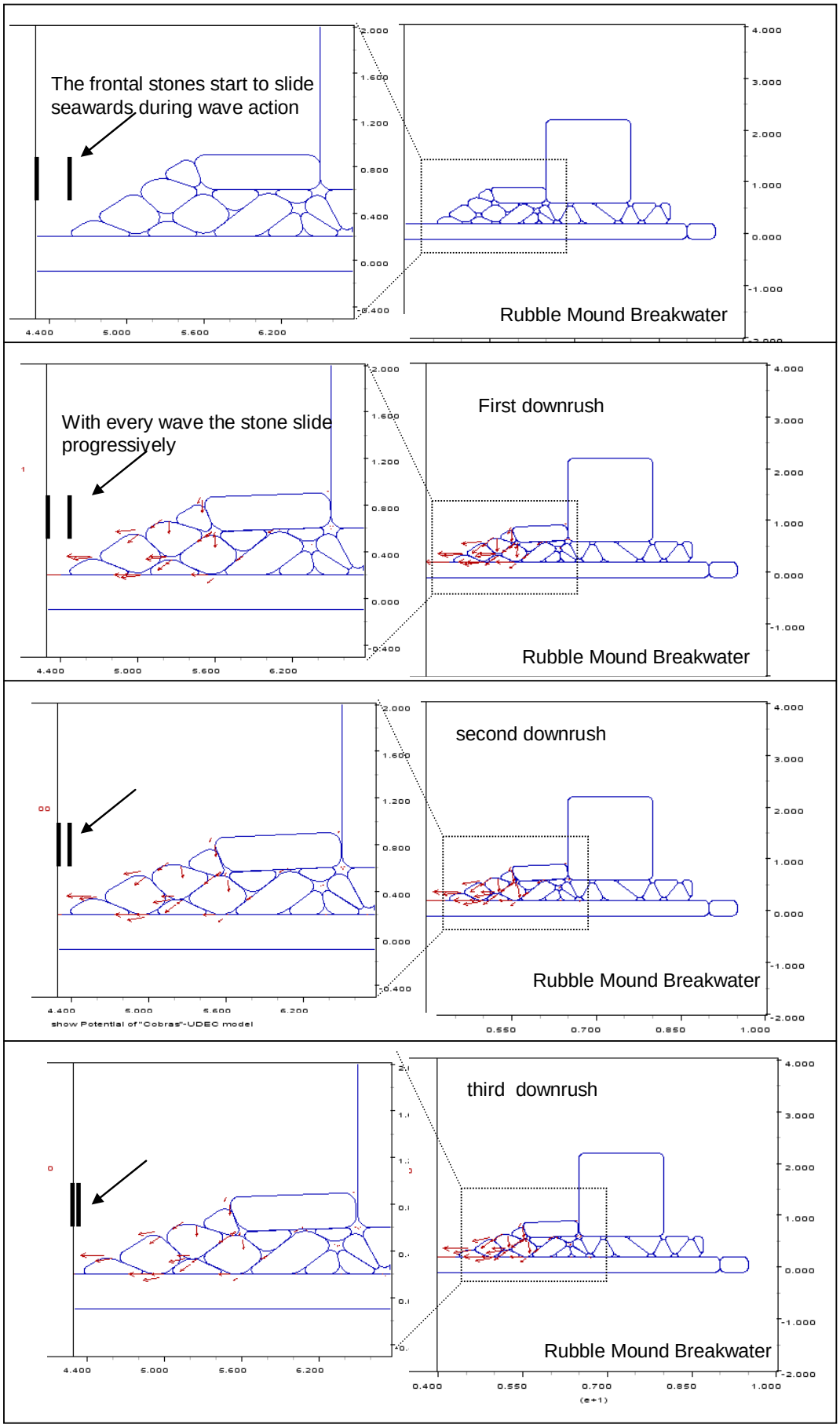

Figure 2: Simulation of a Caisson Breakwater under Wave Action